Synthesis of a bioplastic from agri-food waste

Maria Teresa Miranda Nogueira

Thesis to obtain the Master of Science Degree in

Chemical Engineering

Supervisors:

Dr. Ana Paula da Costa Ribeiro

Prof. Luísa Margarida Dias Ribeiro de Sousa Martins

Examination Committee

Chairperson: Prof. Carlos Manuel Faria de Barros Henriques

Supervisor: Dr. Ana Paula da Costa Ribeiro

Members of the Committee: Dr. Maria Helena Freitas Casimiro

September 2020

Acknowledgement

Firstly, I would like to thank my supervisors – Dr. Ana Ribeiro and Prof. Luísa Martins – for giving me support, ideas and tweak that I needed to continue this project.

Secondly, to Professor Virgínia Infante, professor of the *Departamento de Engenharia Mecânica*, for helping me do the mechanical tests in this work.

Thirdly, I want to thanks to my mom, dad and brother for being there when I went crazy and stressed with the work and foremost for correcting my spelling and my "Portuguese English" overall.

Fourthly, to Inês that was with me through all the experiments and hard work, teaching to use all the new equipment. But, mostly for our "gossip" and the dirty dancing.

And finally, to my friends from university – Pat, Rita and Daniela – for giving advice and be there in all moments of university – bad, good, parties, and so on. To my friends from childhood – Pati and Costa – that reminded me that we are still young and don't need to much stress.

Resumo

O objetivo do presente trabalho foi a criação de um bioplástico a partir de resíduos agro-alimentares, nomeadamente cascas das moscas soldado negro. O passo principal foi a extração da quitina das cascas dos insetos, seguida de sua transformação em quitosano, que é utilizado mais frequentemente em bioplásticos. A extração da quitina foi realizada por desmineralização seguida de desproteinização e descoloração. A sua transformação em quitosano foi realizada por desacetilação. Obteve-se um grau de desacetilação de 71,3 %, o que é superior ao exigido (60 %) para ser considerada quitosano. Todos os produtos foram totalmente caracterizados por microscopia eletrónica de varredura (SEM/EDS), espectroscopia de infravermelho com transformada de Fourier (FTIR) e análise termogravimétrica (TGA).

Para a produção do bioplástico utilizou-se glicerol como dispersante, gelatina ou ágar como ligante, em meio aquoso. A proporção de quitosano e ácido acético (usado para melhorar a solubilidade da quitosano) foi ajustada para obter a consistência desejada. Várias amostras foram produzidas e as selecionadas foram PG33 – feita com agar e 80 % de quitosano – e PG38 – feita com gelatina e 20 % de quitosano. Nestas testou-se o seu comportamento mecânico. A primeira amostra resultou em um filme fino e maleável, enquanto a segunda amostra era mais espessa, permanecendo maleável. Os valores da força de resistência à tração obtidos foram 0,01 e 0,39 N/mm^2, respetivamente.

Também foi possível aumentar a produção por reação (*scaling* up), em escala de bancada, sem perda de semelhança química. Esta é uma etapa importante do processo, pois representa um método potencial para a produção de bioplásticos sustentáveis.

Palavras-chave: Bioplástico, Desperdício agro-alimentar, Quitina, Quitosano

Abstract

The objective of the present work was the creation of a bioplastic from agri-food waste, namely insect exuviae from the black soldier fly. The main step was the extraction of chitin from the insect exuviae, followed by its transformation into chitosan, which is more commonly used in bioplastics. The extraction of the chitin was accomplished by demineralization followed by deproteinization and discolouration. Its transformation into chitosan was achieved by deacetylation. A degree of deacetylation of 71.3 %, was obtained which is higher than the required (60 %) to be considered chitosan. All products were fully characterized by scanning electron microscopy (SEM/EDS), Fourier-transform infrared spectroscopy (FTIR) and thermal gravimetric analysis (TGA).

To produce bioplastic, in an aqueous media, glycerol was used as dispersant, gelatine or agar as a binder. The chitosan and acetic acid (used to improve chitosan solubility) ratio were tuned to obtain the intended consistency. Several samples were produced, and the selected ones were PG33 – made with agar and 80 % of chitosan – and PG38 – made with gelatine and 20 % of chitosan – were tested for mechanical behaviour. The first sample resulted in a thin and malleable film, while the second sample was thicker, remaining malleable. The tensile strength values obtained were 0.01 and 0.39 N/mm2, respectively.

In addition, a successful scaling up, at bench-scale, of the process was achieved. The produced bioplastic at a larger scale was characterized by FTIR and TGA and proven to be identical to the previously obtained. This is a major step in the process, since it represents a potential method to produce sustainable bioplastics.

Keywords: Bioplastic, Agri-food waste, Chitin, Chitosan

Contents

List of Figures

List of Tables

Glossary

A	Agar
B	Biomass
C	Chitin
DD	Degree of Deacetylation
DMSO	Dimethyl sulfoxide
EU	European Union
FTIR-ATR	Fourier Transform Infrared – Attenuated Total Reflectance
FTIR-MIR	Fourier transform mid-infrared spectroscopy
G	Gelatine
HCl	Hydrochloric acid
MW	Molecular Weight
NaOH	Sodium hydroxide
PA	Polyamides
PBAT	Poly (butylene adipate-co-terephthalate)
PE	Polyethylene
PET	Polyethylene terephthalate
PHA	Polyhydroxyalkanoates
PLA	Poly-lactic acid
PP	Polypropylene
PTT	Polyesters
Q	Chitosan
RT	Reaction Time
SEM	Scanning Electron Microscopy
TGA	Thermogravimetric Analysis

1. Introduction

Nowadays, plastics play a big role in making our modern society easier. Plastics are attractive due to their low cost, high durability, flexibility and lightweight, unlike glass, metal or ceramic materials. Plastics allow the creation of a sustainable humanity and develop technology with more efficiency. [1, 2, 3, 4] As we see in the figure 1 "Uses of plastic", plastics are used in different areas, such as in agriculture, packaging and automotive.

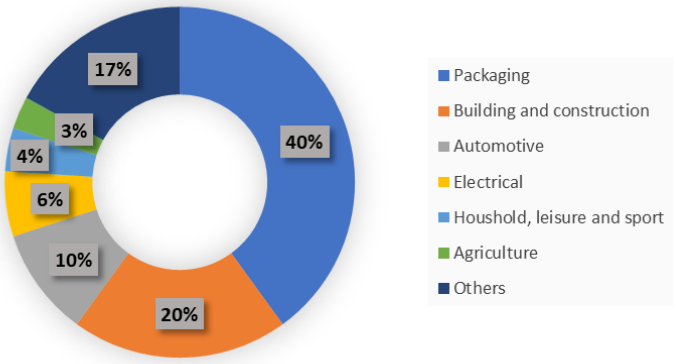

Figure 1 – Uses of plastics. Adapted from [1].

The excessive use of plastic has triggered environmental challenges, like the increase of greenhouse gases emission. It, also, led to the contamination of the ecosystems, including human health, with micro and nano plastics. It also contributed to the increase of municipal solid waste and some countries, in order to reduce the it, burn their plastic waste to generate steam. However, it releases greenhouse effect gases. [1, 2, 5]

Chemists have been developing more efficient ways to recycle or substitute the plastics, because one-third of the total of plastic packaging is still being lost into the environment. So, the life cycle of future plastics must have a more sustainable design. Though, there isn't just one solution for all scenarios, geographies and products. [1, 2, 6] In the figure 2 "Circular economy of plastics" it is possible to see the circular economy for plastics where various methods and technologies of recycling are shown.

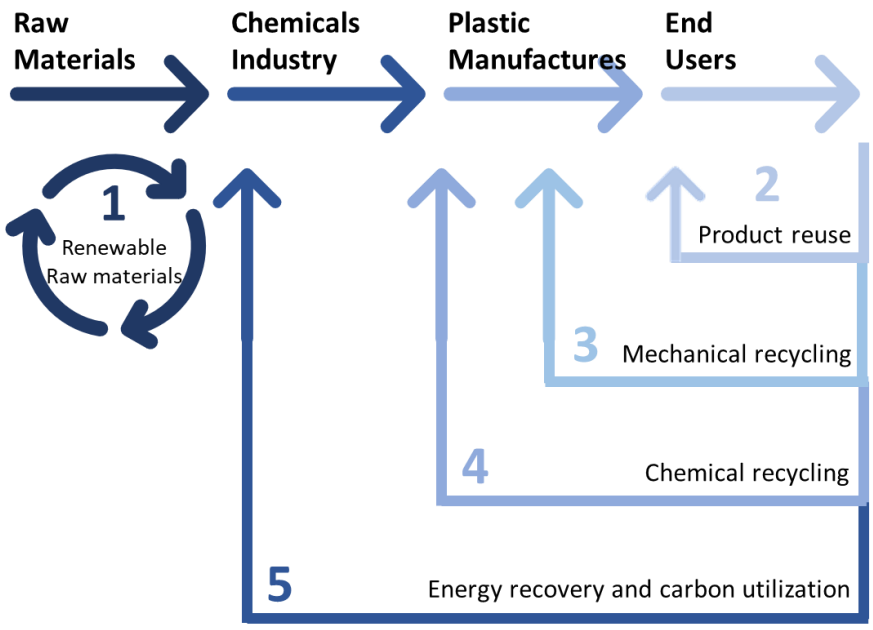

Figure 2 – Circular economy of plastics. Adapted from [1].

Another environmental problem that is happening daily is food loss and food waste. According to the Food and Agriculture Organization (FAO), one-third of the food produced for human consumption is loss or wasted, this corresponds to 1.3 billion tons per year. Food loss happens when it is discarded, incinerated or disposed besides its quality or quantity. On the other hand, food waste occurs when an item is discarded due to its deviates from the optimal conditions, for example, its shape, size or colour. Also, it is necessary to consider that this food waste represents a waste in energy, water, land, soil and other resources that contribute to the increase of green gas emissions. [7, 8]

Combining the food loss and food waste with the necessity to find new ways to substitute the petroleum-based polymers, the bio-based could be a benefit to tackle both. This can be achieved with the help of science, engineering, technology, economies, among others. [2, 9]

Through this work, it will be explained the possible sources of bioplastics, as well as its market. It will also be explained the characteristics of chitin and chitosan, which are the source of the bioplastic produced in this work and, finally, the process used to produce it.

This work aimed to develop a new type of bio-based plastic from a biomass source. The bioplastic was produced using an insect, the black soldier fly exuviae, which is a bioindustry by-product, through laboratory treatments and was chemical, physical and mechanically characterized. Although only produced at a bench-scale it presents the required properties to allow its production to be up-scaled, thus being promising as a material that benefits the environment, by reducing the carbon footprint and improving the ecosystems.

2. Overview of bioplastics

2.1. Definition of bioplastics

Plastics are a polymer, that can have additives, such as stabilizers, plasticizers and flame retardants. Usually, they derive from fossil resources. [1, 5, 6] This is prejudicial for the environment, so the investigators have started to develop bioplastics, as a green alternative.

Bioplastics can be defined as a plastic-like material that is bio-based, biodegradable or both. It is important to know that being bio-based is not the same as being biodegradable. The first one consists on the material coming from biomass, like corn, chitin, sugarcane or cellulose. Being biodegradable means that the microorganisms, such as algae, fungi and bacteria, can convert its components into natural substances, like water and/or carbon dioxide, through a chemical process without the creation of pollution. In spite of being biodegradable, it doesn't depend on the source material to be classified as such. However, it does need optimal environmental conditions to be converted into natural substances. [1, 10, 11, 12, 13]

To classify the most common types of plastics according to its biodegradability and bio-based content there is a graph that synthesis that, which is represented in the figure 3 "Material coordinate system of bioplastics". There is possible to conclude that the most common bioplastics that are bio-based but not biodegradable are polyethylene (PE), polyethylene terephthalate (PET) and polypropylene (PP).

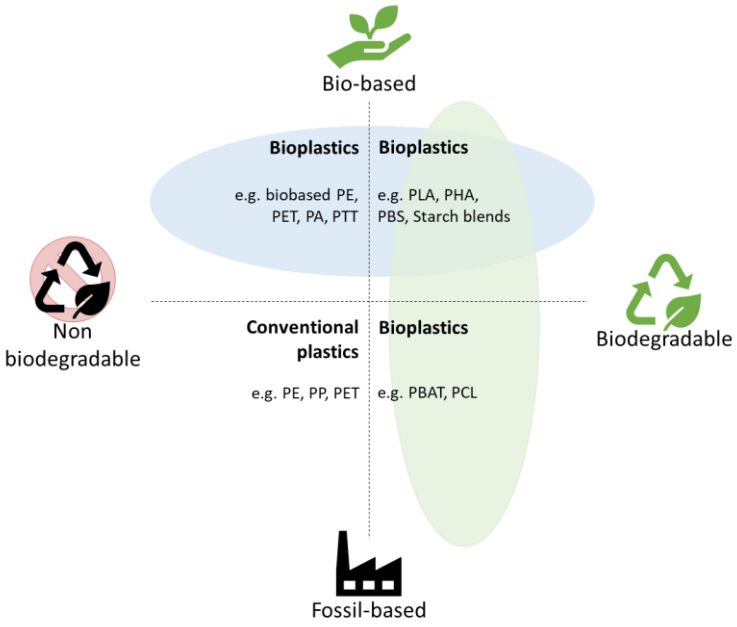

Figure 3 – Material coordinate system of bioplastic. Adapted from [10].

The bioplastics described previously – PE, PET and PP – have a particular characteristic, they can be produced from renewable resources and be identical to their version with a fossil source. These bioplastics are normally used for technical applications and packaging. In the same group, there are the polymers polyamides (PA) and polyesters (PTT). They are considered durable and one of their various application is on textile fibres. [10, 11, 14]

Alternatively, for the group of bio-based and biodegradable the most common bioplastics are poly-lactic acid (PLA) and polyhydroxyalkanoates (PHA). These bioplastics with mixed characteristics are the most recent in the industry and they are mainly used for packaging. [10, 11, 14]

For the group that is biodegradable and fossil-based, the bioplastic poly (butylene adipate-co-terephthalate) (PBAT) is the most common. The bioplastics of this group are usually used with other bioplastics or with starch to improve their applications. [10, 11, 14]

Because the PHA bioplastic has high functionality (mechanic and physical properties) and has a low environmental impact, it has become one of the most likely alternatives for common plastic. It also has biocompatible characteristics. This bioplastic can be manufactured from renewable resources, such as sugars, cellulose, starch and waste products from the agriculture industry. Its weakness is the high cost of production. [15, 16]

Bioplastics have various advantages when compared to conventional plastics, like its reduced carbon footprint. This results in using other sources for its production rather than fossil resources and it has more waste management options, like organic recycling and recovery of the product at its end of life. Although, reducing the emission of greenhouse effect gases, having incentives, like tax benefits, and improved technology, there are some disadvantages. For instance, the unsustainable land use, the scale of production – it only represents 1 % of the 359 million tonnes of plastic produced annually worldwide – and a low level of consumption. [17, 18, 19, 20]

In order to avoid plastic waste accumulation by substituting petroleum-based plastics for bioplastics is mandatory to understand the waste management for these materials. As well as consider the different behaviours and environmental conditions for complete biodegradation of the bioplastics. [5] This leads to the common misperception of the definition of biodegradable and compostable. A material being biodegradable means that it can be broken down by environmental organisms, like bacteria and fungi, in environmental conditions, resulting in its degradation and the release of carbon dioxide and water. This process can take a short or long time and it may or may not leave some toxic residue. On the other hand, a compostable material can be broken down in an artificial environment by a combination of heat, moisture and bacteria, this means that it needs a specific condition to be able to break down. Its results are the release of carbon dioxide, water and inorganic compounds, as

well as some toxic residue. In light of the regulations of the European Union for a plastic being consider compostable, it cannot have more than 10 % of its mass caught in a sieve with a mesh of 2 millimetres after 12 weeks of composting. [1, 21, 22]

In the EU there are certification labels for these plastics. They are classified when the plastics go under standardized tests, like the one previously explained. The figure 4 “Certifications labels for bio-based (left) and compostable (right) plastics” shows the certification labels for the bio-based materials and compostable materials.

Figure 4 – Certifications labels for bio-based (left) and compostable (right) plastics. Adapted from [10].

2.1.1. Bioplastic market

Most products are packaged in plastic containers, so the production of plastic has increased. However, intending to decrease the environmental impact, industries have started to increase the production of bioplastic.

Nowadays, the demand for bioplastics is increasing, leading to the growth and diversification of the bioplastics market. Its production capacity is expected to increase from 2.11 million tonnes in 2019 to 2.43 million tonnes in 2024, in the EU, being the PP and PHA the plastics that have shown the highest relative growth rates. The figure 5 “Global production capacities of bioplastics 2019” shows, in 2019, the biodegradable plastics represented 55.5 % of the global production capacity. Whereas, mixed plastics represented 44.5 %. [1, 20]

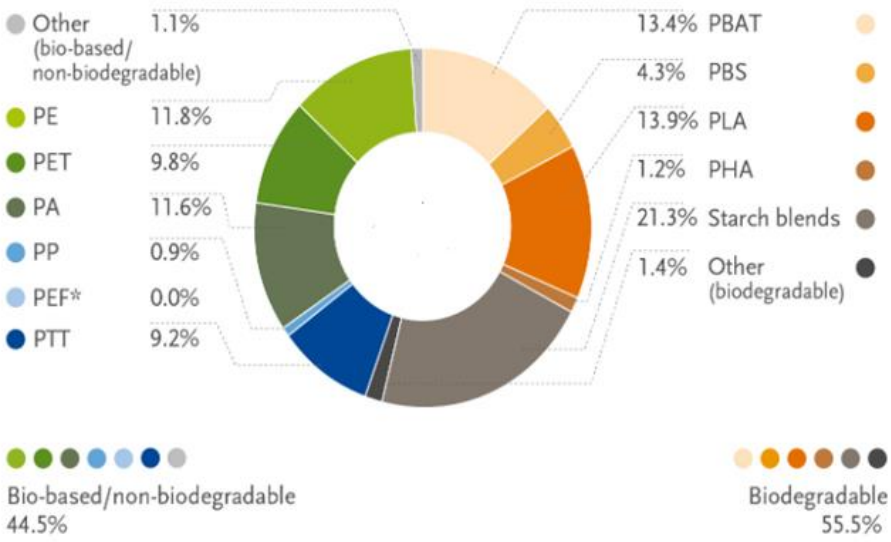

Figure 5 – Global production capacities of bioplastics 2019. Adapted from [1, 20].

Europe represents one-fourth of the worldwide capacity of bioplastics. However, Asia has the major production of bioplastics and regional capacity development.

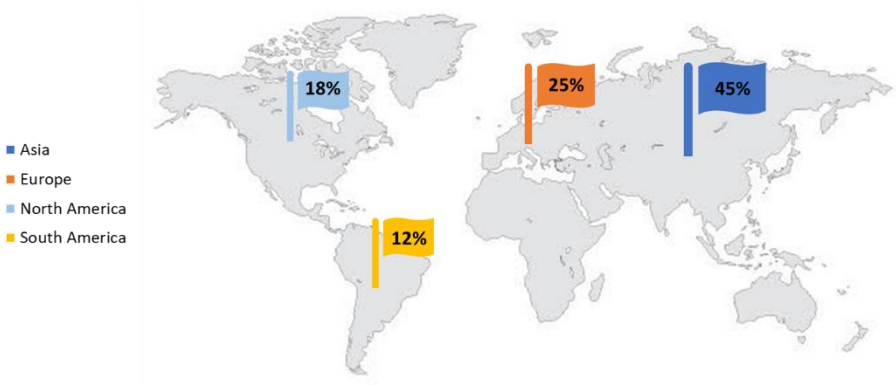

Figure 6 – Global production capacities of bioplastics in 2019. Adapted from [20].

As mentioned earlier, bioplastics have many end-of-life options, such as, reuse, mechanical and chemical recycling and energy recovery. Therefore, bioplastics contribute to the increase of recycling quotas of EU and the implementation of the circular economy. A pros side is visible when the compostable and biodegradable plastics are used as bags or food's packaging. The management efficiency increases due to its possibility of energy production, if there is not a possibility of being reused nor recycled. [23]

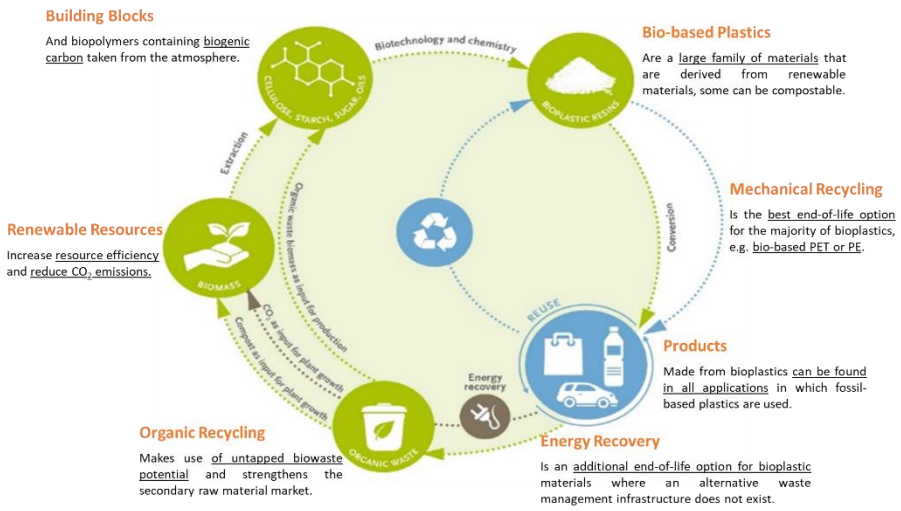

Figure 7 – Bioplastics – closing the loop. Adapted from [23].

Despite, most of the bioplastics being produced from carbohydrate-rich plants, like corn and sugar cane, only 0.02 % of the global agriculture section is used for them. Most of the agriculture section is used for pasture, feed and food. It's also predicted that, in spite of the market growth, this area used by the production of bioplastic stays the same. This demonstrates that there is no competition between the biomass used to produce bioplastics and the biomass used for food and feed. However, there are ways to ensure the supply of the biomass for the different applications, for instance using plant residues to produce bioplastics, improve the efficiency of the conversion of the raw material into feedstock and/or use unplanted land for the agriculture production. [20, 24, 25]

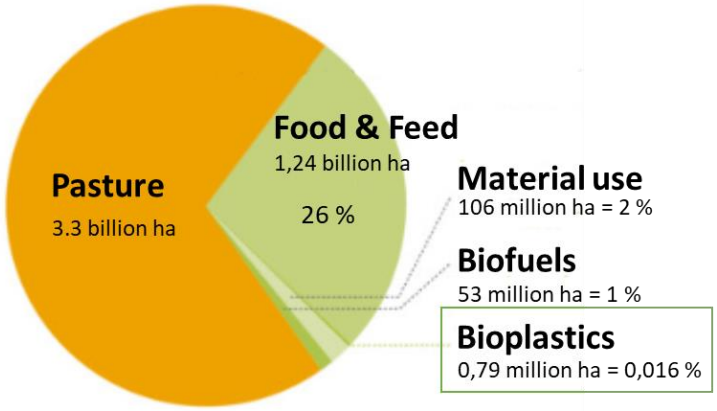

Figure 8 – Estimation of land usage for bioplastics 2019 and 2024. Adapted from [24].

Overall, with the industry moving to a more sustainable and effective future some factors weigh in, for instance, the bioplastics attractive choice, the fact that bioplastics are technologically mature and the society's developed economy and education. [26, 27]

2.2. Chitin

This work aims to produce a bio-based plastic through the biomass chitin. Nevertheless, it is necessary to understand the process of transforming chitin to chitosan.

Chitin is the second most abundant biopolymer in nature just after cellulose. This biopolymer is a natural polysaccharide that is often found in the structural component of crustaceans' exoskeleton and insects, but also in the cells' walls of fungi and microorganisms. The major sources for commercial chitin and chitosan are shrimp, crab, lobster, prawn and krill shells, because they are considered industrial waste and, therefore, are thrown away. [12, 28, 29, 30, 31, 32]

These biopolymers are very attractive for various applications, such as, biomedical, food, chemical and industrial fields. This attention happened because they are biodegradable, biocompatible, non-toxic, eco-safe, renewable and abundant. Also, they are preferred to synthetic polymers because they are cheaper and are present in natural living organisms. [12, 29, 30]

Chitin, as represented in the figure 9 "Chemical structure of chitin", is an acetylated polysaccharide made by N-acetyl-D-glucosamine groups that are linked by β(1-4) linkage. The active groups in chitin are the hydroxyl and free amine groups. [28, 33]

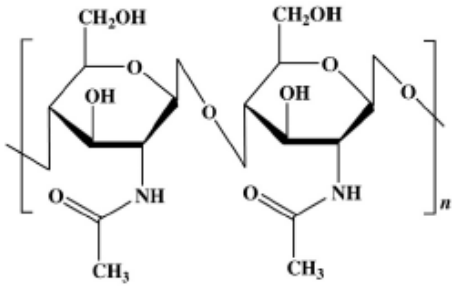

Figure 9 – Chemical structure of chitin. Adapted from [13].

Depending on the raw material, chitin has three allomorphs with crystalline forms – α, β and γ. The difference between these allomorphs is its source. The α-chitin comes from fungi, yeasts, krill, lobsters, crab and insects. This form has an orthorhombic unit with chains arranged in antiparallel sheets or stacks. Whereas, the β-chitin is found in squid pens and it has a monoclinic unit with parallel chains. Lastly, γ-chitin is rarer, but it can be found in the *Ptinus* beetles and Logilo squids. This allomorph has a unit cell with a random chain trend predominating (two up and one down). Because of its antiparallel orientation, α-chitin has a stronger inter and intramolecular bonds that don't allow small molecules into the crystalline phase, so they are preferred for industrial uses. On the other hand, β-chitin has weak intramolecular hydrogen bonds, therefore its solubility, reactivity and swelling can be managed. [29, 34]

The composition of the crustaceans' exoskeleton contains, approximately, 20-30 % of chitin, 30-40 % of protein, 30-50 % of inorganic salts, mainly calcium carbonate and phosphate, and 0-14 % of lipids. [12, 30, 32] Therefore, is necessary to isolate the chitin. Usually, this process needs the consecutive steps of demineralization, deproteinization and discolouration, which are followed by filtration, washing and drying. Usually, before this process, the shells are crushed and washed so the process can be more efficient. [12, 32, 33, 35]

The step of demineralization eliminates the inorganic compounds calcium carbonate and calcium phosphate. This step is processed with diluted acid conditions, the acids usually used are hydrochloric acid (HCl), nitric acid (HNO_3), formic acid (HCOOH), sulphuric acid (H_2SO_4) or ethanoic acid (CH_3COOH), at ambient temperature. In this process, carbon dioxide is released which indicates the removal of mineral content. On the other hand, deproteinization removes protein compounds. This step is processed via an aqueous solution of sodium hydroxide (NaOH) (1-10 %) at 65-100 ºC or via biological fermentative treatments. Finally, in the discolouration step the coloured pigments present in the crustaceans' shells, like astaxanthin, canthaxanthin and beta-carotene are eliminated. This step is done at ambient temperature by solvent extraction, normally with acetone, ethanol, ethyl acetone or their mixtures. [12, 32]

This extraction, with chemical treatments, can have negative consequences, like changing physicochemical properties of the chitin and decrease the molecular weight, as well as the degree of deacetylation. It, also, has a high cost for the purification process of chitin and leads to environmental problems. [30]

Depending on the source the solubility of chitin is altered. However, it is insoluble in common solvents, such as, neutral water, salt solutions and most organic solvents. But is has solubility in ionic liquids, alkali/urea aqueous solution, hexafluoroacetone sesquihydrate, hexafluoroisopropanol chloroalcohols (with sulfuric acid), water mineral solutions and in a mixture of dimethylacetamide with 5 % of lithium chloride. Its insolubility occurs because of its intra- and intermolecular hydrogen bonds that make the polysaccharide dissolved in the solvents indicated. This characteristic has made the chitin attractive for the fabrication of nanomaterial. [12, 29, 33, 34]

2.3. Chitosan

Chitosan, which is represented in the figure 10 “Chemical structure of chitosan”, is a copolymer of glucosamine and N-acetyl-glucosamine groups. The ratio between these two groups is called the degree of deacetylation, which is controlled by modifying the time and temperature of the deacetylation process. Usually, commercial chitosan has a degree of deacetylation between 60 and 100 %. [36] This ratio can determine the degradation rate of the chitosan, as well as, other physiological and biological parameters, like density, solubility, mechanical, barrier and thermal properties. [12, 37, 32]

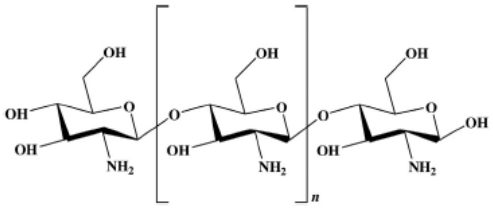

Figure 10 – Chemical structure of chitosan 100 % deacetylated. Adapted from [13].

The chitosan is not highly available in nature, normally it is derived from chitin by the deacetylation process, which frees the amino and hydroxyl groups, which are chemically active, from the chitin. This process involves alkaline hydrolysis of the acetamide groups, and it’s done under a heterogeneous condition with a concentrated base, like NaOH 40-59 % at 100 °C, or under homogeneous conditions at 25-40 °C by freezing-pumping-thawing cycles of an alkaline aqueous suspension of chitin until it dissolves. Other unconventional procedures were developed including the thermomechanical process, flash treatment under microwave dielectric heating, saturated steam and intermittent water washing. [12, 28, 32]

Another influence in the physiochemical and antimicrobial properties of the chitosan is its molecular weight (MW). It can be divided into high molecular weight chitosan, low molecular weight chitosan and oligochitosan – short-chained chitosan. With the rise of the MW the proportion of amine groups and the degree of chitosan chain entanglements increases. This also implies the raise of film forming properties, such as, conductivity, viscosity and surface tension. Chitosan also improves the water barrier property and the tensile strength of the chitosan films. Yet, the membrane permeability alters, affecting the transport of nutrients into the microbial cell membrane and hence in cell lysis. [32]

Chitosan is insoluble in neutral water, in most organic solvents, in sulphuric and phosphoric acid. But it is soluble in dilute acids, like lactic, acetic, glutamic and hydrochloric acid solutions, with a pH up to 6.5. Its lack of solubility occurs because it has low numbers of acetylated groups and due to its primary amino groups, that become protonated, giving it the characteristic of being a strong base.

Nonetheless, when the value of the pH is 6.0 or higher, the polysaccharide becomes insoluble and precipitates due to the deprotonation of the amines. Although the character of the solution affects the chitosan's solubility, its temperature is another determinant factor on its solubility. [29, 32]

Due to the chitosan's free amino and hydroxyl groups, as well as, its derivative formations, phase transformation and polyfunctional alterations can result in matrixes, such as, composites, blends, gels, films and polyampholytes. It also enables the chitosan to have degradability, solubility in weak acids, pH-sensitivity, film-forming properties, biocompatibility, non-antigenic, non-toxicity and low cost. So, its applications are very diverse – as represented in the figure 11 "Chitosan applications" –, it can be used in pharmaceutic, biomedical – in drug delivery, tissue engineering, regenerative medicine –, agriculture, water treatment fields, for preparation of biodegradable films, coatings and nanocomposites; and it has gained some interests in food and paint applications, as well as in the scientific community. [32, 37, 38] Still, it has some limitations, for instance, it is a weak base, has a low affinity with acids, low mechanical strength – it is less flexible and stretchable than plastic films – and it is immiscible in aqueous and many organic solvents. Besides, some chitosan-based materials have higher swelling degree in water. [3, 38]

Figure 11 – Chitosan applications. Adapted from [12, 29].

3. Materials and Methods

3.1. Equipment

Most of the equipment used in this work were easily found in the laboratory environment, such as: a balance from *Mettler Toledo*, a hotplate with a stirrer from *Labox*, an oven from *Indelab*, a muffle from *Snol* and an ultrasound from *Branson 200*. These equipment's were used to do all the proceedings descript in the next sections.

3.2. Raw Materials

The raw material used in this work was the black soldier fly exuviae, from a biomass by-product without any commercial value that is presently considered agricultural waste, which is a rich source of chitin. From it, chitin extraction can be done and the remaining part that did not react can simply be discharged as a compostable material. The insect exuviae is represented in the figure 12 "Biomass with no treatment". This will be mentioned as biomass – B – because it comes from a natural source. The chitin used was donated by a Portuguese company.

Figure 12 – Biomass with no treatment.

It was also used commercial chitosan from *Sigma Aldrich* to compare some of the results of this experiment.

The others raw materials used were easily found in the laboratory, such as, hydrochloric acid 37 % from *Fisher Scientific UK*, sodium hydroxide from *Fisher*, glycerol 99+ from *Alfa Aesar*, agar from *Sigma Aldrich*, acetic acid glacial from *Fisher*, white vinegar, corn-starch gelatine from a local supermarket.

3.3. From chitin to chitosan

The transformation from biomass to chitosan was made following the experiment of the article "A process of preparation of chitin and chitosan from prawn shell waste" (Nessa, F., et al. (2010)) [35]. This process was divided into two parts. The first consists of the extraction of the chitin, which includes the processes of demineralization, deproteinization and discolouration, and the second part is the deacetylation of the chitin.

3.3.1. Part I – Extraction of the chitin from the biomass

First, the raw biomass was crushed and then sifted through a sieve with a mesh of 0.8 mm, as shown in the figure 13 "Fine biomass". This process allowed the following steps to be more efficient.

Figure 13 – Fine biomass.

Then, the process of demineralization was accomplished by adding a 10 % solution of HCl with a solid-to-solvent ratio of 1:10 (w/v) to the fine biomass and was stirred for 22 h at room temperature – RT1 (first reaction time). After, in order to occur the deproteinization, to the previous mixture was added a 10 % solution of NaOH with a solid-to-solvent ratio of 1:15 (w/v) and stirred for 24 h at 70 ºC – RT2 (second reaction time). When finished stirring the mixture was decolourized with acetone and washed with distilled water. (see figure 14 "Process of demineralization (left), deproteinization (middle) and decolourization and washing (right)").

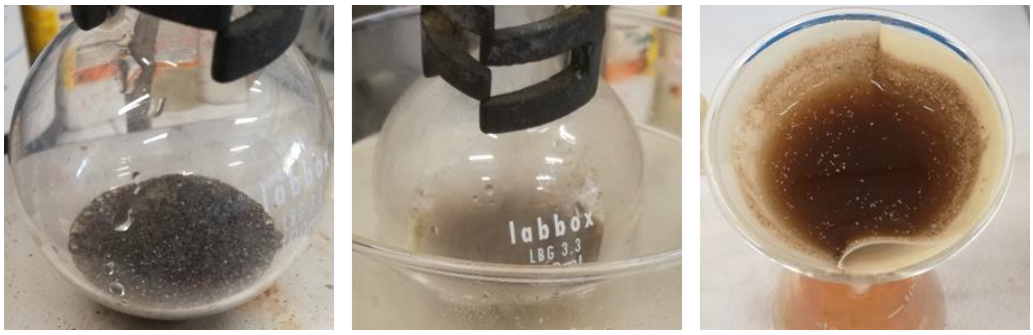

Figure 14 – Process of demineralization (left), deproteinization (middle) and decolourization and washing (right).

The final two steps were a filtration and a complete drying of the product in a stove at 50 ºC.

Figure 15 – Chitin after drying.

The final product of this process is chitin – C (see figure 15 "Chitin after drying").

3.3.2. Part II – Producing the chitosan from the chitin

In order to obtain chitosan, the chitin produced in the part I was crushed and sifted with a sieve with a mesh of 0.8 mm. Then was added a solution of 60 % NaOH with a solid-to-solvent ratio of 1:15 (m/v) and stirred for 72 h at room temperature – RT3 (third reaction time) (see figure 16 "Chitin stirred with a solution of NaOH 60 %").

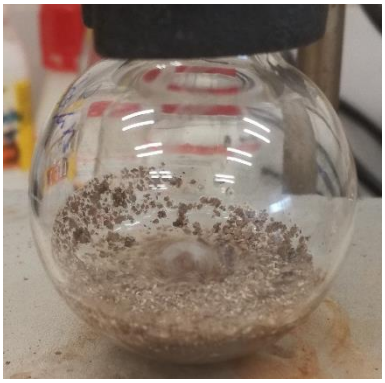

Figure 16 – Chitin stirred with a solution of NaOH 60 %.

To finish this process, the chitosan was washed with distilled water, filtered and dried in a stove at 50 ºC.

Figure 17 – Chitosan after drying.

The final product is chitosan – Q (see figure 17 “Chitosan after drying”).

3.4. From chitosan to bioplastic

3.4.1. Bioplastic 1 – FP

For this experiment was adopted the procedure used by Azevedo, A. *et al.* (2017) [39]. However, instead of using passion fruit or starch as polysaccharide, like the experiment previously mentioned, it was used different polysaccharides, in this case being commercial chitosan, biomass and chitosan. For a dispersant it was used glycerol, and the rest of the components were kept the same – the distilled water, a solution of HCl 0.1M and a solution of NaOH 0.1M.

The quantities used for this process were for one gram of polysaccharide was added 0.4 mL of glycerol, 10 mL of distilled water and 1.2 mL of the solution of HCl 0.1M. The first step was to mix and heat the previous compounds until boiling. Then, with the mixture still on the heat, it was stirred for 20 minutes. Hereafter, the mixture was neutralized with the solution of NaOH 0.1M. The final step is to dry the final product in a muffle at 300 ºC for one hour.

The main changes were the drying process of the polymer, in other words, the drying temperature and time were changed for some samples.

3.4.2. Bioplastic 2 – PG

For these samples the adopted procedure was from Malajovic, M. [40] To prepare this bioplastic for every gram of gelatine – G – was added 2.5 mL of distilled water and 2.5 mL of a solution of 1:20

glycerol. The gelatine aims to work as a binder, whereas the glycerol aims to work as a dispersant. Firstly, the gelatine and the water were heated and stirred until dissolved and the solution becomes more transparent. Afterwards, was added the solution of glycerol, continuing heating and stirring for 10 minutes. The final product was dried on a foil sheet or a petri dish at room temperature in a fume hood, with extraction, for 12 h, until set.

Some changes were made to this process, firstly the gelatine was a substitute for agar – A. In this experiment it was necessary to let the solution agar and distilled water get to a boil and stirred it for 10 minutes, while boiling. Then, to obtain a film that was mouldable, it was necessary to decrease the amount of agar used, maintaining the same quantities of the other compounds. However, the optimal proportion changed, so it was necessary a solution with solid-to-solvent ratio of 1:25 (m/v) of agar and distilled water and for every gram of agar was added 25 mL of the glycerol solution 1:20.

Then, some of the gelatine was replaced by biomass, chitin or chitosan. With the first two products just some of the gelatine was replaced, maintaining the total mass of solids and the same proportion of the distilled water and the solution of glycerol.

On the other hand, when the gelatine was substituted with chitosan, it was necessary to add acetic acid, so that the solution could be homogeneous and alter the process. In this case, the proportion of solid to distilled water and glycerol was kept the same, which means for each gram of solids (gelatine and chitosan) was used 10 mL of distilled water and 0.25 mL of glycerol. Whereas, for each gram of chitosan was used 93.7 µL of acetic acid. With these compounds, three solutions were created, the first was gelatine, made with half of the total distilled water; then, one solution with the glycerol, with one-fourth of the distilled water; and, finally, a solution with the chitosan, having the remaining distilled water and the acetic acid. The process is similar to the original (Malajovic, M), the gelatine was heated and stirred until homogeneous, then the other two solutions were poured in, stirred and heated for 10 minutes. The final step was to dry on a foil sheet or a petri dish at room temperature in a fume hood, with extraction, for 12 h to 48 h, until set.

Another deviation was having agar and chitosan. In this case, the proportion was for each gram of solids (agar and chitosan) the quantity of distilled water added was 11.1 mL and glycerol was 0.28 mL. The proportion of acetic acid and chitosan was kept the same as the previous process, as well as, the experimental method. The only alteration in the method was to boil the solution of agar and distilled water for 5 minutes.

The final two experiments made were by adding magnetite or substituting some of the distilled water with a solution of iron. These experiments were made following the method with agar and chitosan. However, when it was done with magnetite, at the end of the experiment, it was added 5 %

of the total mass of the biomass in magnetite and stirred. In contrast, when the iron solution was added, it was done by substituting some of the distilled water, starting by substituting in the solution with the chitosan and then in the solution with agar.

3.4.3. Bioplastic 3 – BG

To produce the samples BG the method from Wilde, D. (2018) [41] was followed. In this method for each gram of gelatine it is necessary 0.25 g of glycerol and 5 mL of distilled water, then all the previous compounds are mixed and heated until a boil. The final product was dried on a foil sheet or a petri dish at room temperature in a fume hood, with extraction, for 12 h to 48 h, until set.

An experiment was made to this process, switching some of the gelatine for biomass or chitosan. In both changes, just part of the gelatine was substitute in order to maintain the total mass (gelatine plus biomass or chitosan) equal to the mass where it was only the gelatine.

3.4.4. Bioplastic 4 – AMV

Harris, R. *et al.* (2017) [42] developed the experiment as followed, mixing for each gram of corn-starch, 0.3 g of glycerol, 6.7 mL of distilled water and 0.7 mL of white vinegar, let it stir and heat for 10 to 15 minutes and then dried on foil sheet or a petri dish at room temperature in a fume hood, with extraction, for 12 h to 48 h, until set.

An experiment was made with this process, changing some of the corn-starch for biomass. The experimental method was kept the same.

3.5. Analytical Process

3.5.1. Scanning electron microscopy with Energy disperse spectroscopy (SEM/EDS)

This method scans a sample with an electron beam in order to produce a magnified image for analysis. It is performed at high magnifications and generates high-resolution images. The images produced by the SEM are two-dimensional, revealing the texture of the sample and the chemical composition when used with the energy disperse spectroscopy (EDS) feature. Also, it is possible to

analyse selected locations of the images to obtain the composition of the sample. For the equipment to be able to do the analysis, it is necessary to put a slim coat of gold or palladium. [43]

3.5.2. Fourier Transform Infrared (FTIR-ATR)

The main goal of this analysis was to identify the differences between the samples produced during this work with themselves and/or with the theoretical spectrum. The spectrum obtained by this method has a wavenumber between 400 and 4000 cm^{-1}, a resolution of 8, background scans and sample scans of 32. For some samples it was necessary to increase the resolution, the sample scans increased to 132 and the resolution decrease to 4. The software used is the *Microlab PC* from the *Agilent Technologies* company, being the device, also, from the same company.

3.5.3. Degree of deacetylation (DD)

To determine the degree of deacetylation (DD) the Sabin's law (equation 1) was used. This law correlates the degree of deacetylation to the amine and hydroxyl absorption band of the FTIR-MIR spectrum, at 1655 and 3450 cm^{-1}, respectively. [29, 44]

$$DD = 97.67 - \left(26.486 \times \left(\frac{A_{1655}}{A_{3450}}\right)\right) \quad (1)$$

However, to do this calculation the spectrum used was the FTIR-ATR. The difference between the two FTIR's is the preparation of the sample and the way the infrared (IR) beam hits the sample. In the FTIR-MIR method is necessary to create a pallet with potassium bromide (KBr) and the sample. The KBr is used because it is IR transparent. On the other hand, the FTIR-ATR method only requires the sample, without any treatment. Finally, in the FTIR-MIR method, the pallet is placed in the path of the IR beam. Whereas, in the FTIR-ATR the IR beam hits the surface of the sample, only providing chemical information on the functional groups at the surface. [45]

3.5.4. Thermogravimetric analysis (TGA)

This analysis is a destructive technique and is performed by a thermobalance. This equipment registers the mass sample against the temperature or time. [46] In this work, the analysis was made with the variation of the temperature.

All the samples run with a scan rate of 20 °C. Most of the samples followed the action of holding 1 minute at 30 °C; then heating from 30 °C to 750 °C at 20 °C per minute and lastly holding 3 minutes at 750 °C. However, for some samples, the higher temperature was 800 °C and others 900 °C. This happened because the equipment was moved and it was necessary to do some changes.

The software used was *Pyris Software* and the equipment was *Perkin Elmer STA 6000*.

3.5.5. Solubility tests

The solubility tests were made with various solvents such as distilled water, acetone, methanol, ether, ethylene glycol, ethanol, DMSO, chloroform, white vinegar and acetic acid.

3.5.6. pH measurement

The pH was measured with a pH test paper from *Labox*.

3.5.7. Mechanical tests

With the mechanical tests was possible to determine the tensile strength of all the samples and Young's modulus for some of them. This is possible by making bone-like shapes with the bioplastic's samples, so the break could occur in a specific place in which it's known the thickness and the area. It was made three shapes for each sample, when possible, to see if the results were coherent. It was made different on sizes, big, medium and small, with a length of 4.7, 7 or 9.4 centimetres, respectively. The following figures 18, 19 and 20 show the bone's shape made.

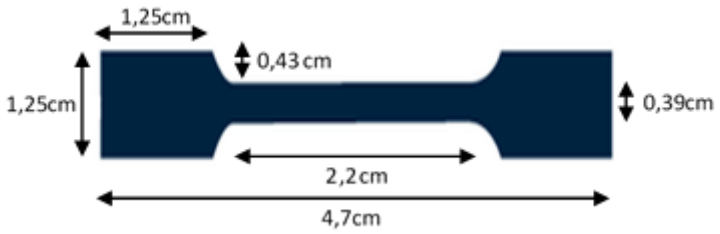

Figure 18 – Bone shape with a length of 4.7 cm.

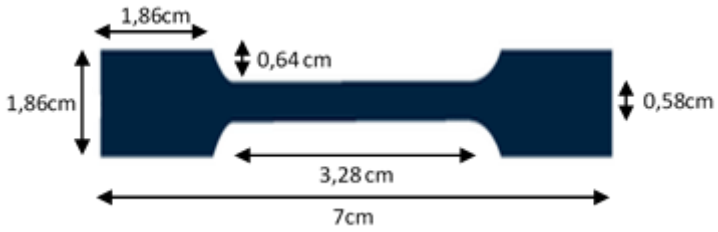

Figure 19 – Bone shape with a length of 7 cm.

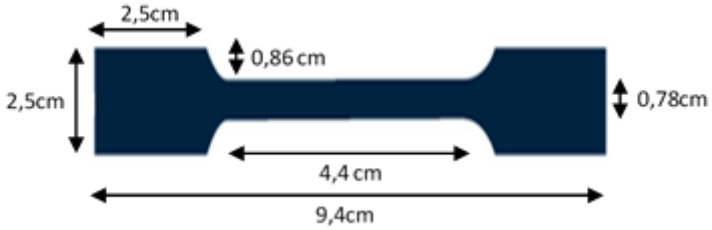

Figure 20 – Bone shape with a length of 9.4 cm.

The equipment used was from *Instron* and the software was *Instron Bluehill*.

Through the equipment is possible to know the extension, in millimetres (mm), versus the load (F), in Newtons (N). Through the equations (2) and (3) is possible to convert the load to tensile strength.

$$\sigma\left[\frac{N}{mm^2}\right] = \frac{F}{A_0} \quad (2)$$

$$A_0[mm^2] = width \times thickness \quad (3)$$

Where σ corresponds to tensile strength and A_0 to the area. The value used for the thickness of the samples was 1 mm and the width were 8.8, 5.8 and 3.9 mm for the big, medium and small sizes, respectively.

On the other hand, to obtain the Young's modulus is necessary to use the equations (4) and (5).

$$\varepsilon = \frac{\Delta L}{l_0} \quad (4)$$

$$E\left[\frac{N}{mm^2}\right] = \frac{\sigma}{\varepsilon} \quad (5)$$

Where ε represents the nominal extension and E the Young's modulus. The value used for l_0 was 20 mm for every sample that was possible to do this calculous. For the ΔL the value depends if the sample suffer from any extension.

3.5.8. Stability tests

These tests were made by putting a piece of a film sample in three balloons with different gaseous atmospheres one was filled with carbon dioxide, the other with nitrogen and the third was left with atmospheric air. Another test was to leave the film under direct sunlight to see if it changes its colour.

4. Results and Discussion

4.1. Biomass

4.1.1. SEM/EDS

Through the SEM image, as shown in the figure 21 “SEM of the biomass”, it is possible to see that the biomass has different features, being some parts are rougher than others. This could be because it comes from an animal, therefore it has not perfect features. It was possible to know that the biomass contains carbon, oxygen, calcium, phosphorus, potassium, magnesium, silicon, sulphur, aluminium and chlorine. It is important to notice that each piece is composed differently, meaning it can all or just some of the components described previously.

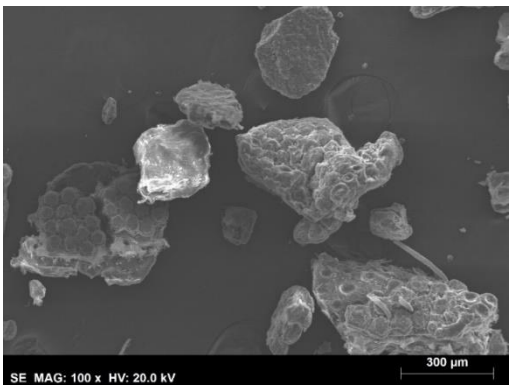

Figure 21 – SEM of the biomass.

4.1.2. FTIR-ATR

In the figure 22 “FTIR-ATR spectra of the biomass (top) and shrimp shell (bottom)” is represented the FTIR-ATR spectrum of the biomass. This was used to be used to compare the transformation of the biomass into chitin. Comparing this spectrum to a spectrum of a shrimp shell (see figure 22) is possible to see that exist some similarities. In the table 1 “Similarities and meaning of the peaks in the biomass and virgin shrimp shell spectrums”.

Table 1 – Similarities and meaning of the peaks in the biomass and virgin shrimp shell spectrums.

Peak biomass	Peak Virgin Shrimp [dd]	Bond
3500 – 3200 cm^{-1}	3500 – 3200 cm^{-1}	• O-H stretching of the water molecule • N-H groups
2919 cm^{-1}	2852 cm^{-1}	C-H stretching vibrations of aliphatic hydrocarbons
1630 cm^{-1}	1653 cm^{-1}	Stretching vibrations of C=O (amide I)
1451 & 873 cm^{-1}	1796, 1456 & 874 cm^{-1}	Stretching and bending vibrations of calcite, $CaCO_3$

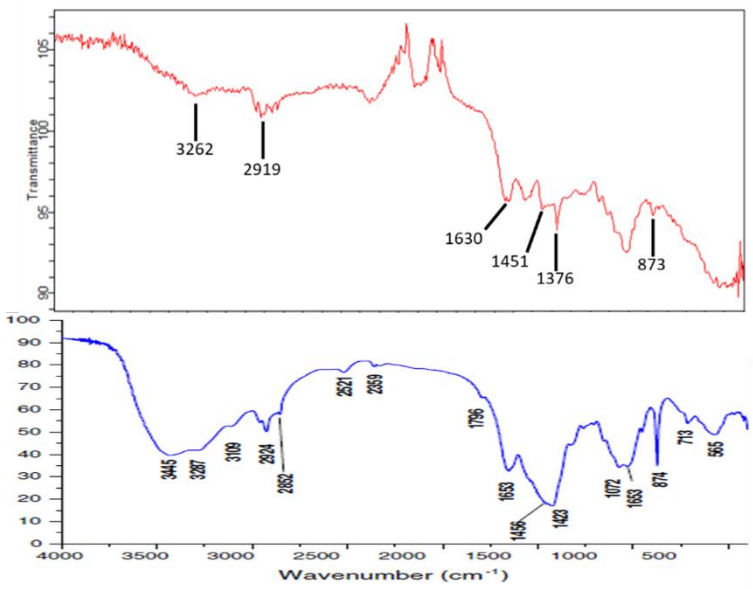

Figure 22 – FTIR-ATR spectra of the biomass (top) and shrimp shell (bottom, adapted from [47]).

Some of the peaks don't correspond because the samples have different characteristics.

4.1.3. TGA

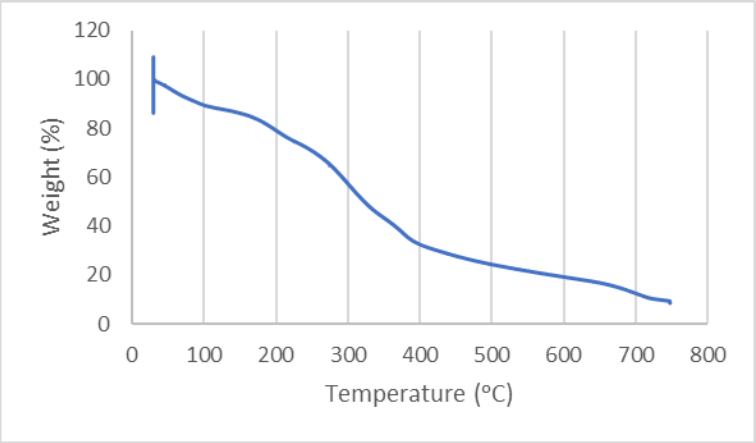

Figure 23 – TGA graph of the biomass.

Through the TGA test (see figure 23 "TGA graph of the biomass") is possible to know that the mass loss for the biomass was 91.5 %, meaning almost all its mass was lost and that it's not very thermally stable. It is also possible to identify some characteristic baselines, such as, until 100 °C is the evaporation of water, from 100 to 400 °C there is a decomposition/depolymerizing of the compound, where some glycosidic bonds are lost, and from 400 until 750 °C there is a thermal degradation and decomposition of carbon residue.

4.1.4. Solubility tests

Some of the biomass was added to distilled water and then put in an ultrasound. In the figure 24 "Solubility test of the biomass in water" is possible to observe that some particles are suspended and the colour of the water changed to brown. Since the biomass did not receive any treatment before its solubility being tested, the change of the water's colour could derive from that.

Figure 24 – Solubility test of the biomass in water.

4.2. From chitin to chitosan

For this experiment, different batches were made, differing the quantity of the biomass and some of the reaction's time, too. Also, some of the batches weren't aiming to produce chitosan, but only chitin, to be used to produce bioplastic in further experiments. In the table 2 "Reaction times for the different batches produced with chitin/chitosan" is possible to know the different reaction times used and if the batch was produced until the chitin or the chitosan.

Table 2 – Reaction times for the different batches produced with chitin/chitosan.

Chitin	Chitosan	Biomass (g)	RT1 (h)	RT2 (h)	RT3 (h)
C1	Q1	0.5	22	24	72
C2	Q2	5.0	22	24	70
C3	Q3	5.0	22	24	80
C4	Q4	2.5	22	24	75
C5	Q5	5.0	66	72	216
C6	-	5.0	22	24	-
C7	-	10.0	22	24	-
C8	Q8	10.0	22	24	72
C9	Q9	75.0	44	72	168

Q1 was the first batch produced, in it were some whitish particles before the last washing and filtration, that were separated, and, after it dried, it created a film with some resistance, as seen in the figure 25 "The final product of Q1".

Figure 25 – The final product of Q1.

It was noticed that, after 2 weeks, Q1 started to curl up and have some white spots, as shown in the figure 26 "Q1 after 2 weeks", in spite of being covered.

Figure 26 – Q1 after 2 weeks.

The next batch made – Q2 – was a scale-up of 10 times to see if the results were the same as Q1. However, as shown in the figure 27 “The final product of Q2”, the final product was not the same, it was easily transformed into dust and was white on the top and brown on the bottom – Q2e and Q2.b, respectively. These two colours were separated to be tested individually. Initially, it was thought that this had happened because the final product was a long time in the stove. Yet, as it will be possible to see further, that was not the case.

The remaining of the experiment steps had similar outcomes as Q1, even the floating whitish particles in the final solution before washing and filtrated.

Figure 27 – The final product of Q2.

Since the result of the sample Q2 was not the expected, Q3 was a replication of it, but with the reaction’s time and drying being closely monitored. Nevertheless, the result was the same as Q2, a white and brown product not a film.

On the other hand, the sample Q4 was made with a scale-up of 5 times regarding Q1. However, upon doing the final wash and filtration, that was left overnight, the product had a jelly-like consistency either on the filtration paper or in the filter – they were called Q4.e and Q4.b, respectably –, as shown in the figure 28 “Q4.e (left) and Q4.b (right) after the last filtration”. The two products were separated and tested individually. After drying in the oven, the product of the filtration paper was light brown and the colour of the filtered was almost see-through.

Figure 28 – Q4.e (left) and Q4.b (right) after the last filtration.

The sample Q5 was made to test if altering the reaction's time, it would modify the result. In this case, the same quantities as Q2 were used and the reaction's time was triplicate. The final product was equal to Q2 and Q3, a white and brown product that is easily transformed into dust.

The batches Q8 and Q9 were produced to be used in the production of bioplastics. The reaction's time of the batch Q9 was different from Q8, that followed the reaction's time of Q1 to Q4, because it had a larger quantity of biomass used. Q9 had another alteration, in the grinding process of the chitin – C9 –, instead of using a mortar it was used a coffee grinder for 30 seconds. Most of the ground particles went through the sieve, the ones that didn't, weren't very big so they were used as is, because the final goal of this batch was to obtain chitosan.

Through this experiment was notice that the time of filtration and drying increases with more biomass, which is expectable.

To calculate the yield of the reaction is necessary for the molecular weight of each compound. However, it was not possible to know this value for the biomass and the value for the chitin and chitosan was a theoretical number. For the chitin, the MW used was 209.19 g/mol and for the chitosan was 1526.5 g/mol.

Table 3 – Yield of the production of chitosan.

Product	Biomass (g)	Chitin (g)	Chitosan (g)	Global Yield (%)
Q1	0.5	0.25	1.03	56.5
Q2	5.0	1.64	8.35	69.8
Q3	5.0	4.25	5.23	16.9
Q4	2.5	1.62	2.81	23.8
Q5	5.0	2.81	9.48	46.2
C6	5.0	2.34	-	-
C7	10.0	7.93	-	-
Q8	10.0	6.23	7.65	16.8
Q9	75.0	45.09	63.51	19.3

The yield values obtained in the table 3 "Yield of the production of chitosan" correspond to the experiment *chitin to chitosan part II*. Starting by comparing the conversion, in mass, of biomass into chitin – experiment *chitin to chitosan part I* – is possible to notice that Q2 has the lower conversion and Q3 has the highest conversion, in spite the reaction's times of these samples were the same. The only samples that had the reaction's time RT1 and RT2 different were Q5 and Q9, still the conversion of biomass into chitin is average. This conclusion is possible to see in the table 4 "Chitin produced for each gram of biomass used".

Table 4 – Chitin produced for each gram of biomass used.

Product	Biomass (g)	Chitin (g)	Product	Biomass (g)	Chitin (g)
C1	1	0.5	C6	1	0.468
C2	1	0.328	C7	1	0.793
C3	1	0.85	C8	1	0.623
C4	1	0.648	C9	1	0.6012
C5	1	0.562			

When comparing the yield of every sample, is possible to notice that Q2 has a higher value and Q8 has the lower, in spite all the reaction times are very similar and the proportion quantity of chitin produced for each gram of biomass being higher in the sample Q8. If we look to the samples Q2 and Q5, that started with the same quantity of biomass, is possible to notice that the proportion of

production of chitin is higher in Q5, but its yield in the production of chitosan is lower. This could mean that to optimize the production of chitin is necessary to increase the reaction time of both reactions, RT1 and RT2, and decrease the RT3 to optimize the yield of the production of chitosan.

Other factors can change the outcome of this experiment, for instance the room temperature is not always the same, this work was developed through the winter and summer. Not all the time, the equipment hotplate with a stirrer used was from the same brand.

4.2.1. SEM/EDS

This analysis was made to the chitin and chitosan. The sample used to the chitin was C3 and for the chitosan were Q1, Q3, Q4.e and Q4.b. For chitosan were tested different samples because the final product for these samples was somewhat different.

From this examination was possible to conclude that the chitin (see figure 29 “SEM of chitin”) had in its composition carbon, oxygen, sodium, calcium, chlorine, magnesium, phosphorus, silicon and potassium. All the elements were expected since they exist in the biomass and/or were added through the process, like the sodium and chlorine.

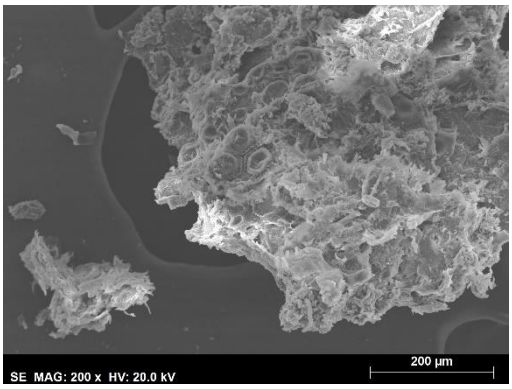

Figure 29 – SEM of chitin.

On the other hand, the analysis made to the different chitosan had a slightly different composition, but all the components were in the composition of the biomass and the chitin. For instance, the sample Q1.p (see figure 30 “SEM of Q1.p”) has present the elements are carbon, oxygen, sodium, calcium, silicon, chloride, aluminium, magnesium and potassium. On the other hand, the elements present in Q3 (see figure 31 “SEM of Q3”) are oxygen, sodium, carbon, calcium and chloride.

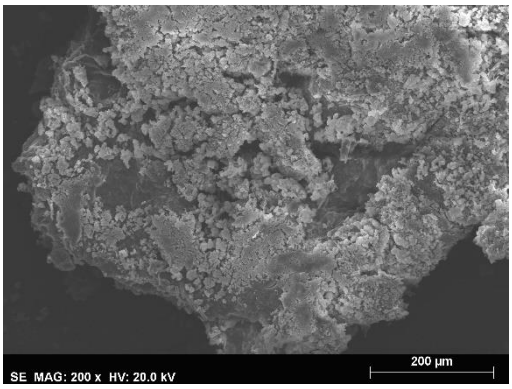

Figure 30 – SEM of Q1.p.

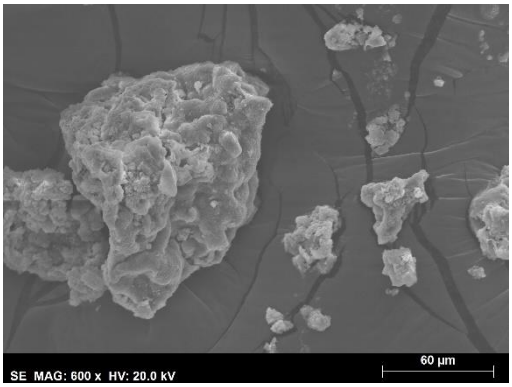

Figure 31 – SEM of Q3.

In the case of Q4, it was tested the jelly-like product in the filtration paper and in the filtrated to see if there is any significant difference. The sample of Q4.e has chloride, carbon, oxygen, sodium, magnesium and calcium. Whereas, Q4.b has chloride, oxygen, carbon and sodium.

Through the analysis of the Q4 (e and b) is possible to see that the magnesium and calcium – originally in the biomass – do not get through the filtration paper, meaning that they are part of the biomass and was not possible to eliminate them.

In the SEM images, there were some different areas within the sample. When comparing the different areas, there were some absent elements. For example, Q3 same areas didn't have chloride. This could be since in the biomass this happens too.

It is important to notice that the device does not detect nitrogen which is expected in the samples.

4.2.2. FTIR-ATR

When comparing the FTIR-ATR spectrum of all the produced chitin (see appendix I.1) is noticed some differences in the peaks that are in the wavenumber between 2500 and 3500 cm^{-1}, which have different intensities, especially in the samples C1, C2, C4 and C5. This can happen due to the different RT's used.

The samples of chitin obtained through this work were compared to a chitin produced with shrimp shell (see figure 32 "FTIR-ATR spectra of chitin from shrimp shell").

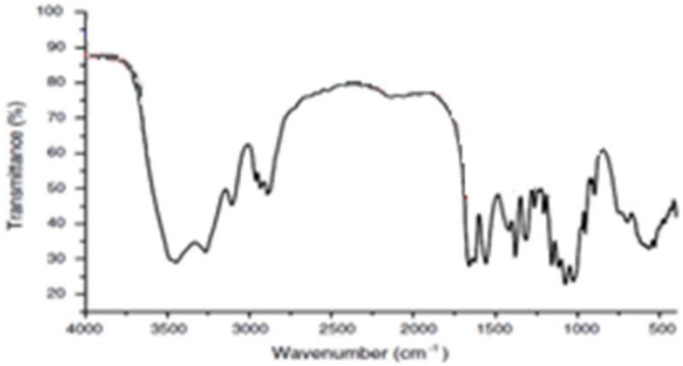

Figure 32 – FTIR-ATR spectra of chitin from shrimp shell. Adapted from [47].

It was possible to conclude that there are some similarities between the various samples, as shown in the table 5 "Similarities and meaning of the peaks in the chitin shrimp and the chitin samples of this work spectrums".

Table 5 – Similarities and meaning of the peaks in the chitin shrimp and the chitin samples of this work spectrums.

Wavenumber (cm^{-1})										
Chitin shrimp	**C1**	**C2**	**C3**	**C4**	**C5**	**C6**	**C7**	**C8**	**C9**	**Bond**
3500 - 3100	3243	3255	3340 & 3255	3255	3258	3337 & 3255	3258	3255	3266	O-H and NH groups
2934	2919	2915	2923	2923	2923	2919	2919	2919	2919	C-H stretching vibrations (CH_2 & CH_3)
1661 & 1626	1648 & 1618	1656 & 1622	1641 & 1622	1645 & 1622	1641 & 1622	1652 & 1622	1637 & 1622	1641 & 1622	1641 & 1618	C=O secondary stretch (amide I)
1559	1555	1563	1559	1548	1559	1544	1540	1540	1540	NH bend, CN stretch (amide II)
1416	1410	1410	1399	1376	1402	1402	1402	1399	1402	CH_2 bending & CH_3 deformation

1312	1313	1309	1309	1309	1309	1320	1313	1313	1313	CH_2 wagging (amide III)
1157	1153	1153	1156	1153	1156	1156	1153	1153	1153	Asymmetric bridge oxygen stretching
1074	1041	1041	1059	1059	1059	1041	1044	1048	1044	C-O-C asymmetric stretch in phase ring
1028	1026	1026	1026	1022	1011	1022	1026	1022	1022	CO stretching
897	873	877	873	873	873	873	873	869	869	CH stretching (saccharide rings)

The two peaks that correspond to the amine I indicate that the chitin extracted from the biomass is in α-form. [47]

With the chitosan's spectrums (see appendix I.2) the differences noticed were in the same peaks as the chitin. The Q1 was compared when recently made and after 2 weeks drying. Both spectra have the same peaks, however, the 2 weeks film peaks are more accentuated and more intense. On the other hand, when comparing Q2.b with Q2.e, is possible to see that the first sample doesn't have a big peak at 3500 cm^{-1} like the second sample, but the remaining peaks are similar. This also happened with the sample Q4.e and Q4.b, but the Q4.e was the sample that doesn't have the peak at 3500 cm^{-1}.

As the chitin samples, the chitosan samples were also compared to a chitosan done with shrimp shell [48] (see table 6 "Similarities and meaning of the peaks in the chitosan shrimp and the chitosan samples of this work spectrums").

Table 6 – Similarities and meaning of the peaks in the chitosan shrimp and the chitosan samples of this work spectrums.

	Wavenumber (cm^{-1})											
Chitosan shrimp	**Q1.b**	**Q1.p**	**Q1.p 2 week**	**Q2.b**	**Q2.e**	**Q3**	**Q4.b**	**Q4.e**	**Q5**	**Q8**	**Q9**	**Bond**
3500 - 3100	3273	3217	3165	3392	3299	-	-	-	-	-	-	O-H and NH groups
2920	2919	2919	2975	-	2923	2923	2945	2919	2856	2919	2923	C-H stretching vibrations (CH_2 & CH_3)
1659	1641	1641	1652	1663	1630	1589	1667	1600	1626	1633	1630	C=O secondary stretch (amide I)
1420	1410	1440	1413	1410	1410	1421	1432	1421	1421	1421	1425	Axial deformation of the C-N of the amide

1319, 1360 & 1379	-	-	1354	-	1335	1335	1387	-	-	1339	1335	Strong vibration of the bending of the -NH primary, secondary and tertiary
1060	-	1026	1071	1071	1018	1018	1071	1018	1018	1011	1018	C-O-C asymmetric stretch in phase ring
896	877	866	866	881	862	877	862	881	881	881	877	CH stretching (saccharide rings)

Through the spectrums is possible to see a decreasing of the intensity of the peak at 1659 cm^{-1}, which corresponds to the process of deacetylation. [48]

The deviation of the wavenumber, between the chitin/chitosan form the shrimp and the chitin/chitosan produced in this work, can happen because the samples are not the same.

The chitosan commercial, which was used in some experiments, was compared with the obtained chitosan. Through the FTIR-ATR spectrums (see appendix I.2) was noticed that they are similar, the only difference is the intensity of the peaks.

Finally, when the spectrums of the chitin and chitosan are compared to the biomass is possible to see some changes, mainly the intensity of some peaks and the change of others, which is expected, because there are creation and breakage of some chemical bonds.

4.2.3. DD

In the table 7 is represented the value of the degree of deacetylation of each chitosan sample.

Table 7 – Degree of deacetylation of each chitosan sample.

Sample	Q1.p	Q1.b	Q2.b	Q2.e	Q3	Q4.b	Q4.e	Q5	Q8	Q9
DD (%)	72.1	71.4	71.1	70.3	71.5	71.1	71.3	71.1	71.7	71.2

The average value of the degree of deacetylation is 71.3 % with the method FTIR-ATR.

The Sabin's law was also applied with the values obtained in the FTIR-MIR spectrum of Q9 to see if there is any alteration. The conclusion is that the DD of this sample is 43.7 %, which corresponds to an error of 39 %. However, the spectrum has a lot of noise, which is possible to see in the figure 33

"FTIR-MIR of Q9", which can lead to deviations in the intensity of the peaks. This noise can be an outcome of the humidity present in the sample or the KBr.

When compared to the value obtained in this work with Casadidio, C. *et al.* (2019) [29] – 73.5, 82.3 and 82.5 % – is possible to notice that they are lower, with a difference of 10 %.

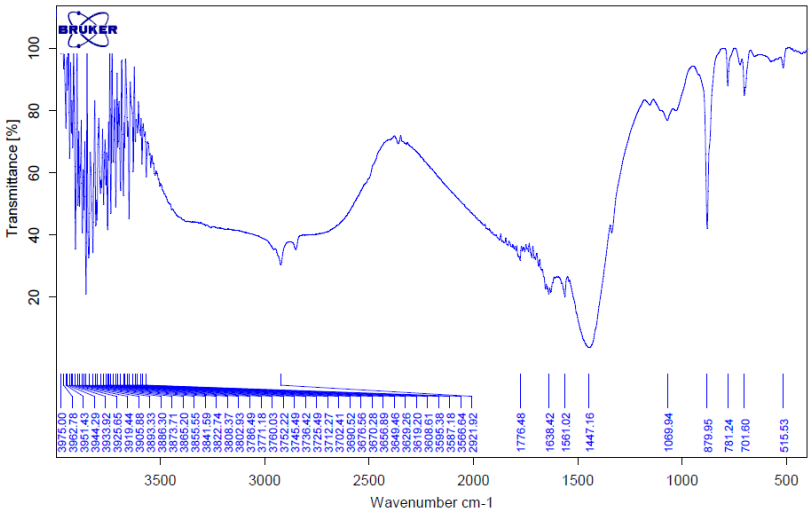

Figure 33 – FTIR-MIR of Q9.

4.2.4. TGA

The TGA analysis was made only to one sample of chitin – C7 – and chitosan – Q5 (see figure 34 "TGA graph of C7" and figure 35 "TGA graph of Q5", respectively).

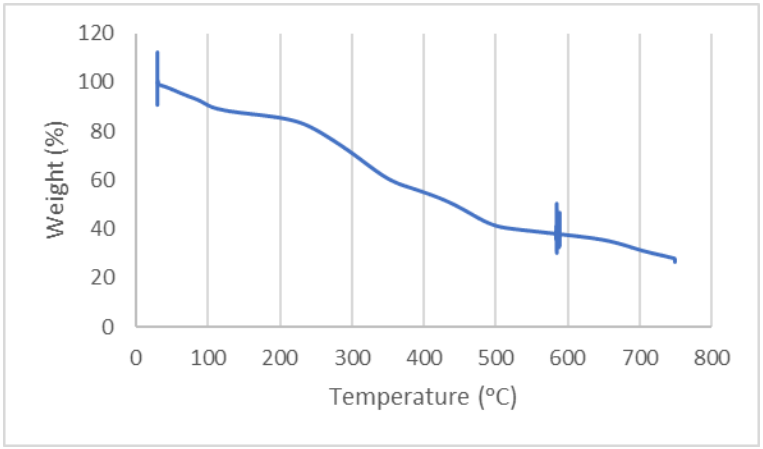

Figure 34 – TGA graph of C7.

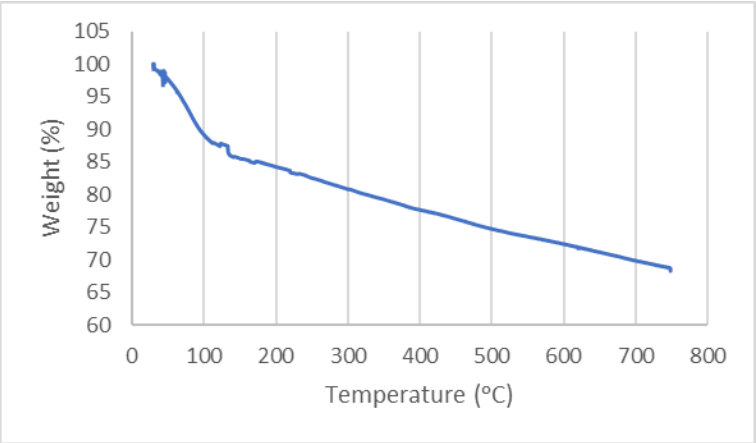

Figure 35 – TGA graph of Q5.

As seen in the previous graphics the mass loss of C7 and Q5 was 73.5 % and 31.8 %, respectively.

In the TGA graph of the chitin and the chitosan is possible to see that is loss of water until the temperature of 100 °C. On the other hand, just in the chitin TGA graph there is a thermal degradation happening at 500 °C, approximately. Whereas, in the chitosan exists a depolymerization and a decomposition from 200 °C until 750 °C.

Through mass loss of the products, biomass, chitin and chitosan, is possible to conclude that throughout the treatments they are becoming thermally more stable.

4.2.5. Solubility tests

The solubility tests made to the chitosan commercial were with the solvents chloroform and DMSO. As shown in the figure 36 this product is not soluble in any of the solvents.

Figure 36 – Solubility test to chitosan commercial with chloroform (left) and DMSO (right).

To the Q1 film was done a solubility test with the solvents distilled water, acetone, methanol and ethanol. It is possible to see in the figure 37 that did not dissolve in any solvent and in the water it floats.

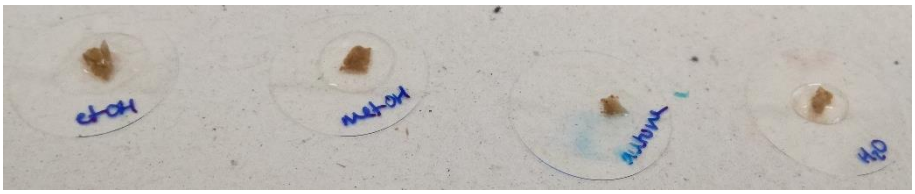

Figure 37 – Solubility test to Q1 with ethanol, methanol, acetone and distilled water (left to right).

It was tested the Q2 product – the white and brown particles – solubility in distilled water, ether, ethylene glycol and ethanol. As seen in the figure 38 the white Q2 is soluble in water and ethylene glycol. However brown Q2 is not soluble in any solvent, as shown in the figure 39.

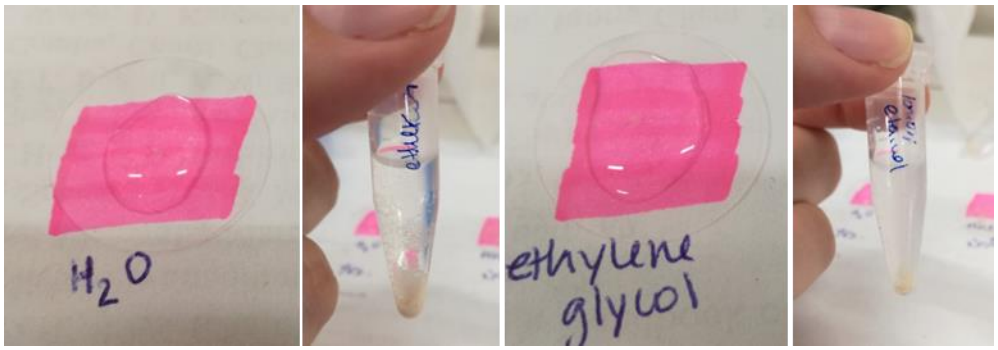

Figure 38 – Solubility test to white Q2 with distilled water, ether, ethylene glycol and ethanol (left to right).

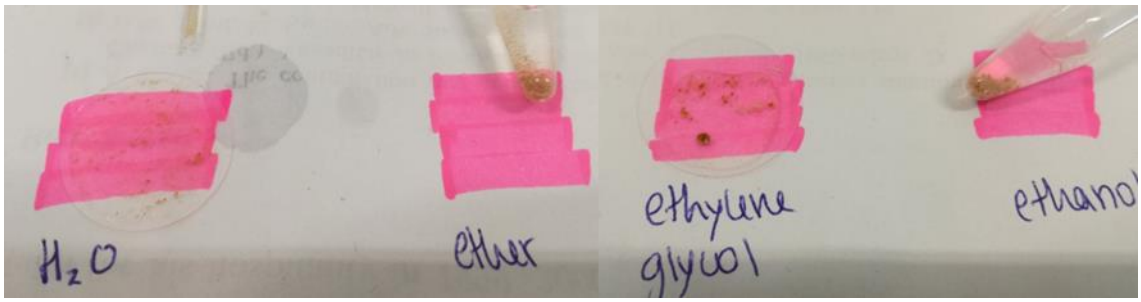

Figure 39 – Solubility test to brown Q2 with distilled water, ether, ethylene glycol and ethanol (left to right).

It was also made a solubility test to Q3 with distilled water, ether, ethylene glycol and ethanol. As exposed in the figure 40, Q3 just have some solubility in distilled water.

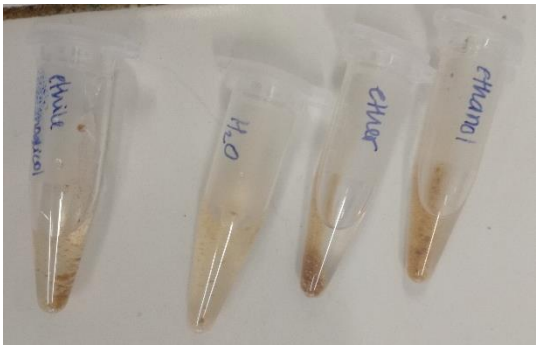

Figure 40 – Solubility test to Q3 with ethylene glycol, distilled water, ether and ethanol (left to right).

Another test of the solubility of chitosan was made with Q5. In this case, the test was made with a solution of acetic acid 1 and 2 % and white vinegar. In the figure 41 is possible to see that the chitosan is soluble in every solution tested. However, it is possible to notice that with the solution of acetic acid there are some particles of chitosan left.

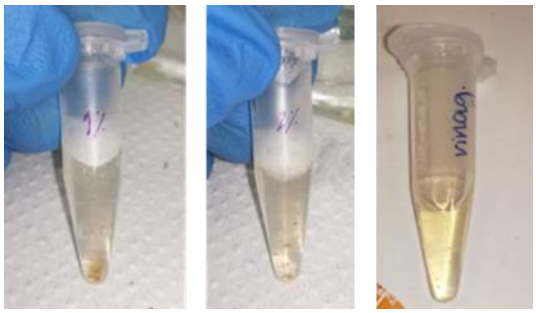

Figure 41 – Solubility test to Q5 with a solution of acetic acid 1 and 2 % and white vinegar (left to right).

4.2.6. pH measurements

Through the experiment of producing chitosan, the pH was measure with a pH test paper. In the first reaction, the pH was 1. When added de NaOH 10 % the pH was 8. The final product has a pH of 10.

4.3. FP

The first experiment – FP1 – was made with commercial chitosan. When comparing the solution before and after it went to the muffle (see figure 42 "FP1 before (left) and after (right) it went to the oven") is possible to notice that the solution looks thick and almost translucid before, whereas, after the final treatment, it becomes hard and black.

Figure 42 – FP1 before (left) and after (right) it went to the oven.

Like the previous sample, FP2 was made with commercial chitosan, however, it was left to dry overnight at 50 °C in the stove, instead of 300 °C oven for 1 hour in the muffle. After it dried overnight, it looked like a loose polymer, so half of the sample was pressed (see figure 43 “FP2 after drying in a 50 °C (left) stove and in a 130 °C (right) muffle”) to see if it would hold its shape after drying for 1 hour at 130 °C in a muffle. The result was yellow and is loose dust that didn’t hold its shape.

Figure 43 – FP2 after drying in a 50 °C (left) stove and in a 130 °C (right) muffle.

To test this method, FP3 was produced with biomass and, as expected, some changes were noticed. For instance, before the sample dries in the stove, it had a brown colour and it was liquid. It was also noticed that the sample was not homogeneous (see figure 44 “FP3 after drying in a 50 °C (left) stove and in a 130 °C (right) muffle”). This sample had the same drying process as FP2, but it didn’t harden after this process.

Figure 44 – FP3 after drying in a 50 °C (left) stove and in a 130 °C (right) muffle.

The sample FP4 was like FP2, but with the double of dispersant and it only dried in the stove at 50 °C overnight. The results, before and after drying, are similar to FP2, it is possible to press the polymer, but it doesn’t hold it shape (see figure 45 “FP4 before (left) and after (right) dying in a 50 °C stove overnight”).

Figure 45 – FP4 before (left) and after (right) dying in a 50 °C stove overnight.

The sample FP5 was made with biomass, like FP3. However, it was dried in the muffle at 130 °C for one plus one hour. Through the figure 46 “FP5 after drying 2 hours in a 130 °C muffle”, the result was a drier product than FP3.

Figure 46 – FP5 after drying 2 hours in a 130 °C muffle.

To test experiments using chitosan, FP6 and FP7 were produced with Q2 white and brown, respectively. Both samples were divided to test the drying process, one part dried in an oven at 50 °C for 1 week and the other at 300 °C for 1 hour. The sample that dried at 300ºC charred, the other continues with a liquid look (see figure 47 “FP6 (down) and FP7 (top) before (left), after drying at 300 °C (middle) and after drying at 50 °C (right)”).

Figure 47 – FP6 (down) and FP7 (top) before (left), after drying at 300 °C (middle) and after drying at 50 °C (right).

To see what happens if the drying time changed, FP8 and FP9 like FP6 and FP7, respectively. For these samples, the drying time was 1h30min at 130 °C in the muffle. As shown in the figure 48 “FP8 (left) and FP9 (right) after drying at 130 °C in the muffle the first (top) and second (bottom) time”, the product of FP8 was a fragile film and the FP9 had a paste-like consistency. However, after 12 h at room temperature, the samples turned liquid, so they have dried again for 1h30 at 130 °C and the result was a fragile film for FP8 and paste-like consistency for FP9.

Figure 48 – FP8 (left) and FP9 (right) after drying at 130 °C in the muffle the first (top) and second (bottom) time.

FP10 was made like FP8, but the quantity of glycerol used was doubled and it dried for 1 h at 130 °C. On the other hand, FP11 was made with Q3 with the same quantities as FP8 and dried at the same time as FP10. The result of these samples was the same as FP8 and FP9, they turned liquid after 12 h from drying in the oven (see figure 49 “FP10 (left) and FP11 (right) after drying in the muffle (top) and after resting on the bench (bottom)”).

Figure 49 – FP10 (left) and FP11 (right) after drying in the muffle (top) and after resting on the bench (bottom).

Finally, FP12 was made with Q4. This sample was dried in a muffle at 130 °C for 1h30 plus 1h30. The final product was dried but didn't become a film, as demonstrated in the figure 50 "FP12 after the first (left) and second (right) time drying at 130 °C for 1h30 in the muffle".

Figure 50 – FP12 after the first (left) and second (right) time drying at 130 °C for 1h30 in the muffle.

4.3.1. SEM/EDS

This analysis was made only to the sample was FP8 (see figure 51 "SEM of FP8") – produced with chitosan. The components present in this sample are chloride, carbon, oxygen, sodium and silicon.

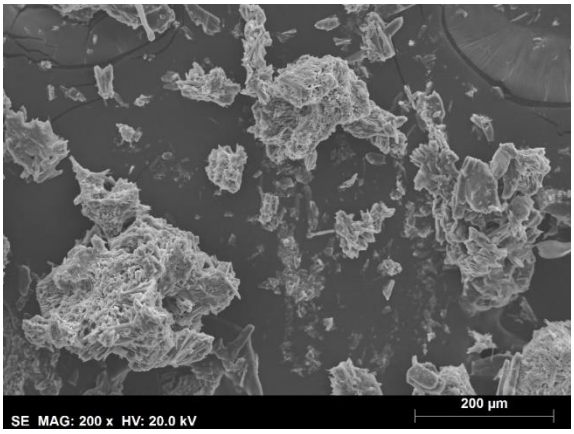

Figure 51 – SEM of FP8.

4.3.2. FTIR-ATR

For this experiment, the samples were compared by the polysaccharide used (see appendix I.3 for the spectrums). For instance, when comparing FP1, FP2 and FP4, that was used commercial chitosan, is possible to conclude that all the spectrums are similar, just the FP2 that was dried in the stove versus the one dried in the muffle have a difference in the intensity of the peak at 3250 cm^{-1}. This difference can occur due to its dryness.

On the other hand, the sample FP5, that what used biomass as polysaccharide, when compared with the spectrum of the biomass, has some differences in the peaks located between 3500 and 2250

cm^{-1}. This can mean that there were some changes in the composition between the sample and the biomass, as well as, the FP5 has more water content. Lastly, the sample FP5 that was dried 1 h in the muffle and the one that was dried 2 h, don't have differences in their spectrums.

Additionally, the samples made with chitosan – FP6, FP7, FP8, FP9, FP10, FP11 and FP12 – have some differences between 3500 and 2500 cm^{-1}, mainly their intensity, as expected because of the dryness of the samples. However, the biggest difference noticed was in the samples FP6 and FP7 dried in the stove for 1 day, in contrast with 1 week. In the spectrum of the samples only dried for 1 day there are almost no peaks in the range of values previously mentioned, this can happen because the mixture didn't react completely, whereas after 1 week the reaction was completed.

Lastly, three peaks are constant throughout the spectrums. The first peak is located between 3500 and 3100 cm^{-1}, which corresponds to O-H and NH groups. The other peaks are located at 1660 and 1420 cm^{-1} that correspond to the amide I and the axial deformation of the C-N of the amide, respectively.

4.4. PG

The samples PG1 to PG3 were made following the original experiment, using 2 g of gelatine, and PG34 with 6 g of gelatine. PG2 diverges from PG1, because it was used the double of glycerol. Whereas PG3 and PG34 were made with the same formulation as PG1 but dried in a thinner coat. Comparing the first two samples it is noticed that PG2 is more bendable then PG1 and PG3 become a hard film, but not crisp.

The samples PG4, PG5, PG8, PG16, PG18 and PG20 were made with agar, following the process mentioned in section 3.4.2. In the table 8 "Different quantities of agar used for each study sample" are discriminated against the quantities of agar used for each test.

Table 8 – Different quantities of agar used for each study sample.

Sample	PG4	PG5	PG8	PG16	PG18	PG20
Agar (g)	0.2	1.0	0.1	0.2	0.5	0.25

The difference between PG4 and PG16 is in the last one the mixture came to a boil for 10 minutes. From this study is possible to conclude that with more agar the film becomes very hard and not mouldable. On the other hand, not boiling the mixture make it shader after dried – figure 52 "PG4 (left)

and PG16 (right) after drying for 1 week at room temperature". In this test, the best result was obtained with 0.2 g of agar.

Figure 52 – PG4 (left) and PG16 (right) after drying for 1 week at room temperature.

The samples PG6, PG7, PG9 to PG15 and PG17 were made with gelatine and biomass, following the method explained in section 3.4.2. In the table 9 "Percentage of biomass for each sample" is possible to find the percentage of biomass used and in the figure 53 "Each test with biomass after drying" is represented the results after drying the samples.

Table 9 – Percentage of biomass for each sample.

Sample	PG6	PG7	PG9	PG10	PG11	PG12	PG13	PG14	PG15	PG17
% of biomass	90	10	80	20	70	30	60	40	50	85

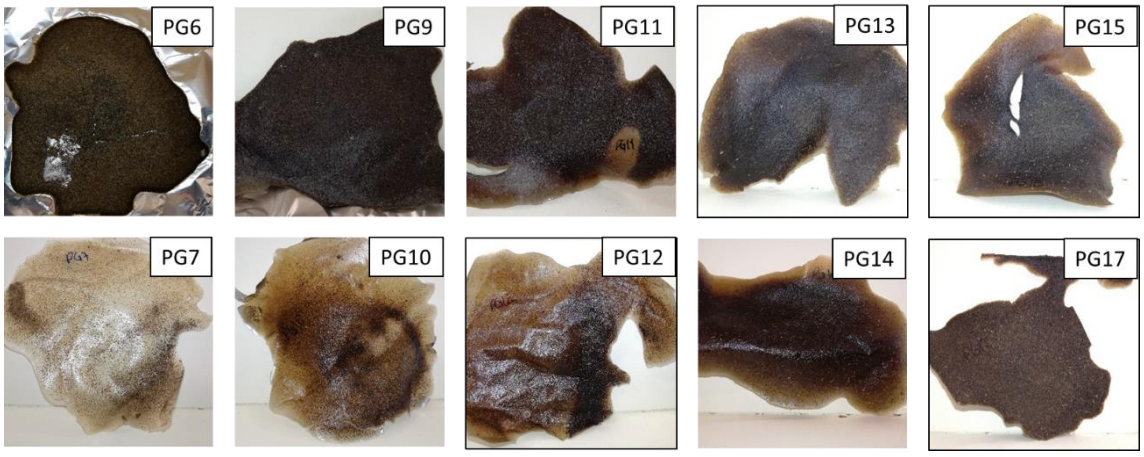

Figure 53 – Each test with biomass after drying.

In the figure 53 is possible to see that the less biomass the samples has the more the dispersion is noticeable. In these tests the only one that didn't form a film was PG6, which corresponds to a higher percentage of biomass. On the other hand, PG11 and PG15 had a crack, this can happen, because of the surface they dried on or room temperature. Finally, PG17 was the sample that had the most biomass that forms a film without cracking and is uniform. So, it was used as a reference to do other

tests when substituting the biomass for chitin or chitosan. All these samples had a bad smell to it, this happens, because the biomass is a raw product from an animal without any treatment.

The tests PG19, PG21, PG22, PG35 and PG38 were made with chitosan and gelatine. The tests PG19, PG21 and PG22 (see figure 54 “PG19, PG21 and PG22 after drying”) didn’t have acetic acid incorporated. So, the first test – PG19 – was made with 2 g of solids, being 80 % of chitosan, following the process for the sample gelatine and biomass. The result was one big piece that had hardened and a liquid that after drying it transformed into dust. On the other hand, PG21 in the same way as PG19, but the chitosan was added slowly to avoid the separation of the film. For this sample, it was used 0.13 g of chitosan, but it was made as if it was used 2 g of solids. The result was a moist film and not homogeneous. Finally, PG22 was made by following the process of chitosan and agar explained in section 3.4.2. without the acetic acid and with the same proportions as PG19. The product had a crumbly texture and didn’t form a film.

The samples PG35 and PG38 (see figure 55 “PG35 and PG38 after drying”) were made by following the method with gelatine and chitosan explained in section 3.4.2. Both samples were made with a total of solids of 6 g. However, PG35 was made with 80 % of chitosan and PG38 with 20 % of chitosan. The product of PG35 was a very thin and malleable film. Whereas PG38 had a thicker consistency, but it was also malleable.

Lastly, all these samples, with chitosan and chitin, didn’t have an unpleasant smell, because the chitosan is a treated compound.

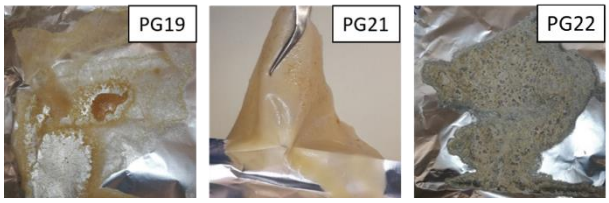

Figure 54 – PG19, PG21 and PG22 after drying.

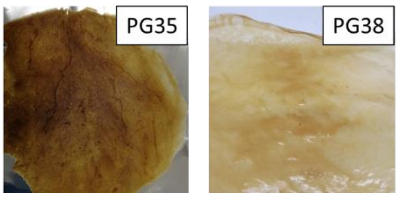

Figure 55 – PG35 and PG38 after drying.

The sample PG23 (see figure 56 “PG23 after drying”) was made with chitin and gelatine, following the method explained in section 3.4.2. for this combination. This sample was made with a total of 2 g of solids which 85 % was chitin. This sample after 48 hours still had a moist look, so it had to dry for 4

days in the fume hood, with extraction. The result was a film that on the top is matt and on the bottom is shiny.

Figure 56 – PG23 after drying.

It was also tested biomass with agar – sample PG37 – with a total mass of 4.8 g of biomass. For this sample were made two tests, because in the first attempt the heating time the agar with water was lower than normal and the result was not the expected. However, when repeating the test with the heating time correct the result was the same, a film with multiple cracks (see figure 57 “PG37.2 after drying”).

Figure 57 – PG37.2 after drying.

The samples PG24 and PG36 were made with chitin and agar. For the first sample, it was used 1.8 g of chitin, whereas for the second was used 2.9 g of chitin. After drying, FP24 had shrunk and had formed a film with some resistance. On the other hand, PG36 is a film with multiple cracks (see figure 58 “PG324 and PG36 after drying”).

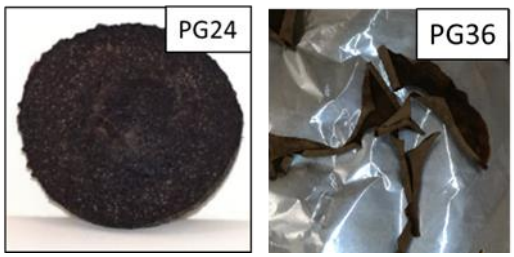

Figure 58 – PG324 and PG36 after drying.

To test the chitosan with agar the samples PG25, PG26, PG27, PG30, PG33, PG33.2 and PG33.3 (see figure 59 “PG25, PG26 (PG26.f on the left and PG26.c on the right), PG27, PG30 and PG33 after

drying") were produced, following the method explained in the section 3.4.2. and with acetic acid. In the first test – PG25 – it was used 1,6 g of chitosan and the quantity of acetic acid used was less than the used for the next samples, in this case, it was used 50 µL of acetic acid, despite the solution had some dispersion. The result was a hard shell that looks it crystalized. So, PG26 was produced with the proportion of acetic acid explained previously. This sample was separated into two petri dishes, in one of them, the film was thin and in the other, it was thicker. When dried, the thin film – PG26.f – becomes a film with some resistance and had a light colour. On the other hand, the thicker – PG26.c – form crystals at the top and had some humidity, but it looks like a film.

PG27 and PG30 were made to test if the solution handles more chitosan, following the method explained previously, they were made with 1.8 and 2 g of chitosan, respectively. These two samples were made like PG26. PG27 resulted in a film, that on the top is white and had some spots brown and doesn't have flexibility. While, PG30 is harder than the PG26 and PG27, but still flexible and it formed a white spot. All these samples shrunk after drying. Finally, the last sample with chitosan and agar made was a scale-up of PG26 of 3 times – PG33, PG33.2 and PG33.3. PG26 was chosen to repeat the test because it had the best results when done with a fine coat. The result was 23 centimetres film. However, because it didn't dry enough time it was difficult to take from the plate and it broke into several pieces.

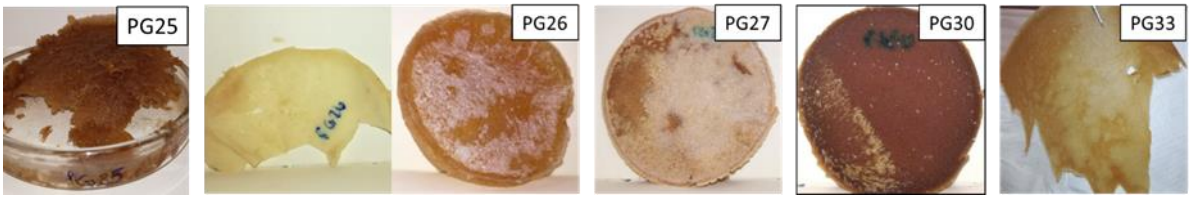

Figure 59 – PG25, PG26 (PG26.f on the left and PG26.c on the right), PG27, PG30 and PG33 after drying.

The sample PG28 was made to test the addition of magnetite into the solution. The product had the suspension of the magnetite and didn't change the formation of the film (see figure 60 "PG28 after drying").

Figure 60 – PG28 after drying.

Finally, the last test made was by substituting the distilled water with a solution of Fe^{2+}. Three tests were made by substituting 5 (PG29), 25 (PG32) and 50 % (PG31) of the distilled water, these tests were made by following the process mentioned in section 3.4.2. Although the solution of Fe^{2+} is purple, when it was added to the sample PG31 turned brown. This means that the Fe^{2+} changed to Fe^{3+}. All the samples prepared with this solution had a big spot on the top that crystalize (see figure 61 "PG29, PG31 and PG32 after drying").

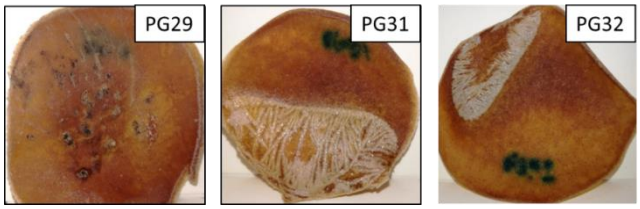

Figure 61 – PG29, PG31 and PG32 after drying.

4.4.1. SEM/EDS

This analysis was made to the samples PG3, PG17, PG23 and PG33. The first sample was made only with gelatine, the second with gelatine and biomass, the third with gelatine and chitin and the fourth sample was made with agar and chitosan.

The compounds found in the sample PG3 were carbon, oxygen, silicon, sulphur, chloride and cerium. Also, through the figure 62 "SEM of PG3" is possible that the surface of the film has some droplets that can be expected, because of the water used in this process.

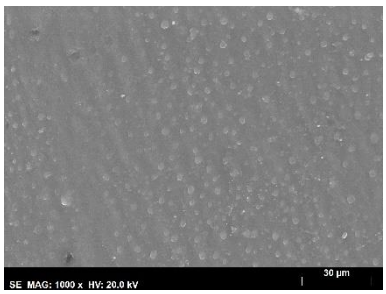

Figure 62 – SEM of PG3.

Whilst, PG17 has the compounds oxygen, calcium, carbon, potassium, silicon, magnesium, phosphorus and sulphur. Then, PG23 has carbon, chloride, sodium, oxygen, calcium, sodium, potassium, phosphorus, magnesium, silicon, sulphur and aluminium. On the other hand, in the sample PG33, there are carbon, oxygen, sodium, calcium, chloride, silicon and magnesium. These compounds were expected for all the samples, because they all exist in the polysaccharide.

4.4.2. FTIR-ATR

All the spectrums of these samples can be found in the appendix I.4.

When comparing the samples PG1, PG3 and PG34, which were made with gelatine, is possible to notice that the spectrums are very similar. The only difference found is on the spectrum of PG34, where the peak at 3525 cm^{-1} is less intense, this could happen, because of the different quantity of gelatine used or the time it was drying may have changed. If the spectrums of these samples are compared with gelatine (see figure 63 "FTIR-ATR spectra of PG38 (top) and gelatine (bottom)"), they are very similar until the wavenumber 1500 cm^{-1}. Which is also expected since the samples have other components to them. PG1 and PG2 have a mild difference in the peak at 1000 cm^{-1} that may be caused by the increase of glycerol used.

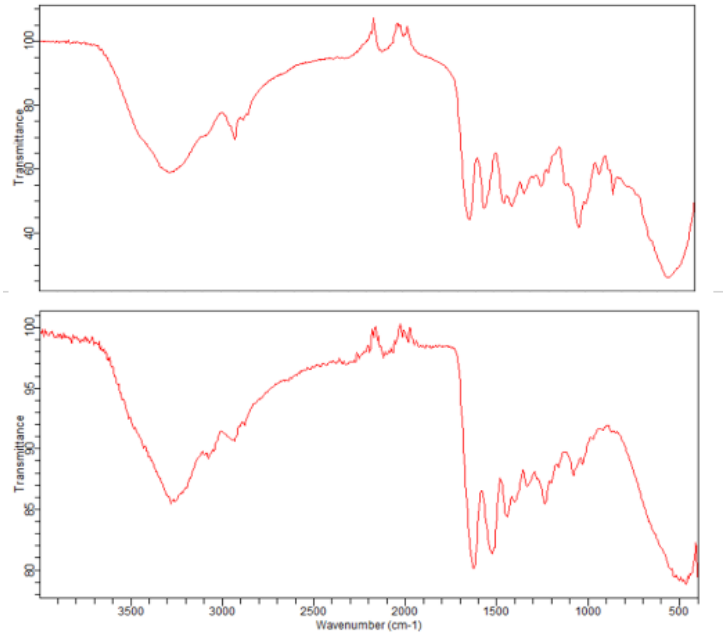

Figure 63 – FTIR-ATR spectra of PG38 (top) and gelatine (bottom).

Whereas, the samples PG4, PG5, PG8, PG16, PG18 and PG20, made only with agar, were compared with the spectrum of agar (see figure 64 "FTIR-ATR spectra of PG33 (top) and agar (bottom)") and it is possible to notice that they differ in the wavenumbers between 1500 and 400 cm^{-1}. On the other hand, the samples PG4, PG8, PG16 and PG20 have very similar spectrums. This can happen, because the mass of agar used is very similar for each sample. Whereas, PG5 and PG18 differ from PG4 in the peaks around 3500 cm^{-1} and 1500 cm^{-1}. These two samples have more agar and that can change the spectrum.

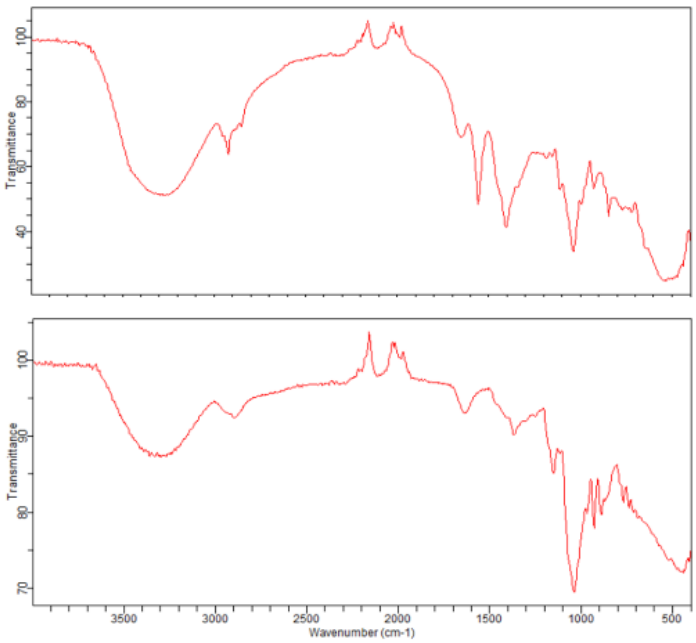

Figure 64 – FTIR-ATR spectra of PG33 (top) and agar (bottom).

In the case of the samples made with biomass and gelatine, the samples PG6, PG9, PG11, PG13 and PG17 have similar spectrums, because they correspond to the samples with a higher content of biomass. On the other end, PG7, PG10, PG12 and PG14 have similar spectrums for the same reason as the previous samples. The sample PG15 is a combination of the previous spectrums, since it has 50 % of each component. All the samples have the peaks at 3500 and 1500 cm^{-1} that corresponds to the gelatine and the peak at 500 cm^{-1} that corresponds to the biomass. Like the sample PG23 also has a peak at 3500 cm^{-1} that corresponds to the gelatine.

Within the samples made with gelatine and chitosan, the sample PG19, which is divided into the hard shell and dusted film, has a difference in the peaks at 1500 cm^{-1}. This can happen, because most of the gelatine went to the hard shell and most of the chitosan went to the dusted film. Between the samples PG21 and PG22 exist a difference in the peaks at 1500 cm^{-1}, where it is more intense in the sample PG22, which has more chitosan. Lastly, the samples PG35 and PG38 also differ in the peak with the same wavenumber as the previous ones, where the spectrum of PG35 is similar to the chitosan, which makes sense, since it has more quantity of it.

The sample PG37, which was made with agar and biomass, has a spectrum with a combination of the spectrum's agar and biomass, as expected. On the other hand, the sample's spectrums of PG24 and PG36, which were made with agar and chitin, are very similar and are a combination of the spectrum of chitin and agar.

All the samples made with agar and chitosan – PG25, PG26, PH27, PG30, PG33, PG33.2 and PG33.3 – are very similar to each other. The only difference is between the PG26 that dried in a thin layer and the PG26 that created some crystals in the surfaces, being the peak at 1500 cm^{-1} in the PG26.f less intense.

Between the spectrum's samples made with the solution of Fe^{2+} – PG29, PG31 and PG32 – there are no differences. Meanwhile, the sample PG28, that was made with magnetite, didn't change the spectrum from PG26, that is the magnetite doesn't change the chemical bonds in the film.

Finally, like the experiment PG three peaks are constant throughout the spectrums. The first peak is located between 3500 and 3100 cm^{-1} and the other two peaks are located at 1660 and 1420 cm^{-1}.

4.4.3. TGA

The mass loss percentages of some samples of PG are in the table 10 "Mass loss percentage of some samples of PG".

Table 10 – Mass loss percentage of some samples of PG.

Sample	PG3	PG6	PG7	PG9	PG10	PG11
% loss	93.5	82.9	92.3	82.1	80.6	86.2
Sample	PG16	PG23	PG26.f	PG28	PG29	PG33
% loss	96.2	78.3	80.0	51.6	55.0	61.8

Through the table 10 is possible to see the major PG's samples have a high degradation, regardless of its polysaccharide. Except for the sample PG28 and PG29 that were made with a solution of Fe^{2+} and magnetite, respectively. Which is expected because there is an accumulation of residue coming from the metal present in the samples.

4.4.4. pH measurements

The pH measured for some examples is explicit in the table 11 "pH of some samples of PG" and is possible to conclude that most of the samples are neutral to alkali.

Table 11 – pH of some samples of PG.

Sample	PG7	PG9	PG10	PG11	PG12	PG13	PG14	PG15	PG16	PG17
pH	8	8	7	8	7	8	7	9	9	8
Sample	PG24	PG25	PG26	PG33	PG34	PG35	PG36	PG37	PG39	
pH	8	7	9	9	7	10	9	7	10	

4.4.5. Mechanical tests

The main comparison done with the mechanical tests were between the tensile strength of some samples. Firstly, in the figure 65 "Tensile strength vs % of gelatine in the sample with gelatine and biomass", was compared the samples that have gelatine and biomass. It is possible to see that there is no linear comparison between the tensile strength and the percentage of gelatine present in the sample. So, the quantity of biomass used in the sample can be optimized in order to have a better result. Also, it is noticed that the sample with only gelatine have a higher tensile strength value.

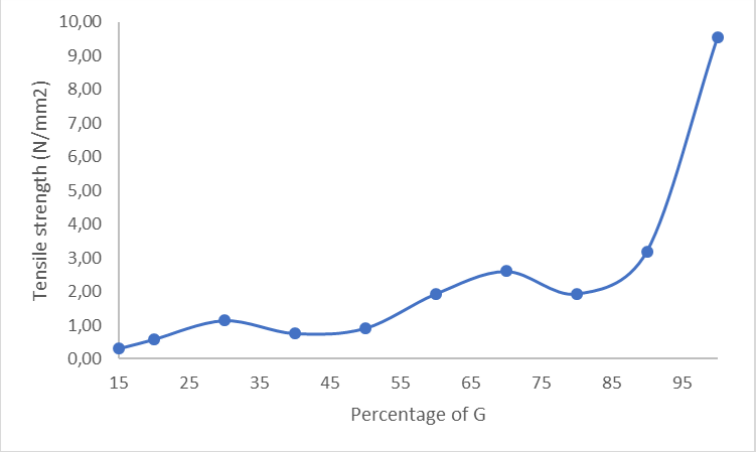

Figure 65 – Tensile strength vs % of gelatine in the sample with gelatine and biomass.

On the other hand, when the samples made with gelatine and biomass, chitin or chitosan were compared is possible to notice that the higher value corresponds to the sample with only gelatine (see figure 66 "Tensile strength vs Sample with polysaccharide and gelatine"). Then, the samples PG17, PG23 and PG35 have the same quantity of gelatine substitute, but they don't have similar results. However, when comparing the first two samples with the sample PG38 they have similar results, that is when the samples have both gelatine and chitosan, it is necessary to increase the amount of gelatine to obtain a higher value of tensile strength.

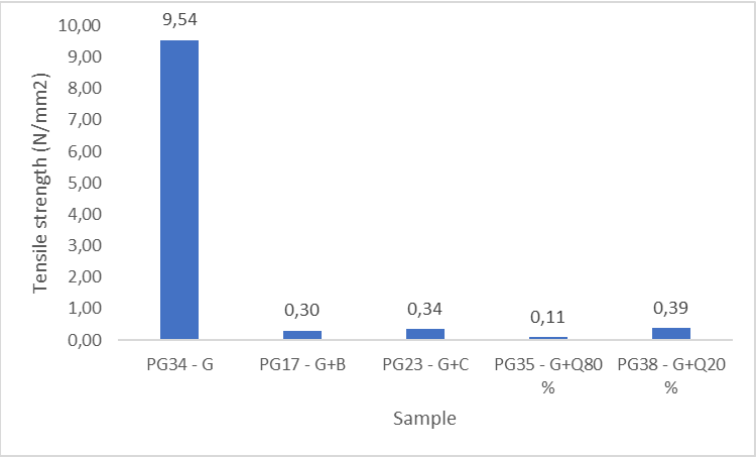

Figure 66 – Tensile strength vs Sample with polysaccharide and gelatine.

The final evaluation done with the tensile strength was with the samples with agar (see figure 67 "Tensile strength vs Sample with polysaccharide and agar"). In this case, if there's a polysaccharide added to the mixture the tensile strength decreases. This can happen because the chemical bonds can change with the addition of some compounds.

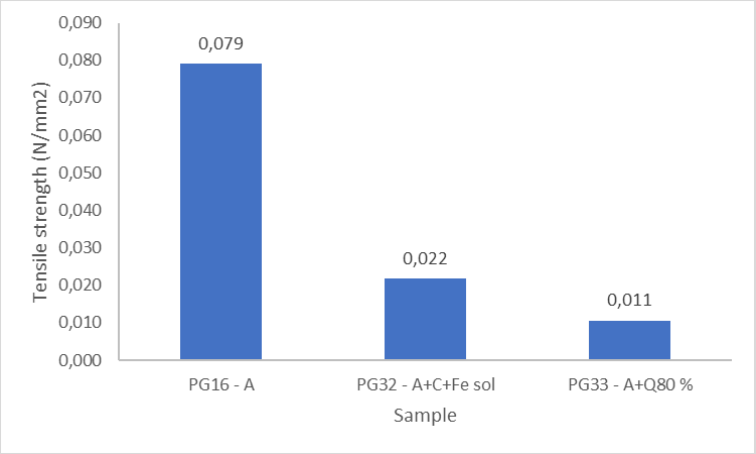

Figure 67 – Tensile strength vs Sample with polysaccharide and agar.

To calculate the Young's modulus is necessary that the film stretches and maintains that elongation. For most samples, this did not happen, so it was only possible to calculate this value for the samples discriminated in the table 12 "Young's modulus for each sample".

Table 12 – Young's modulus for each sample.

Sample	PG7.a	PG7.b	PG13.b	PG15.b	PG15.c	PG33
E (N/mm²)	140.37	97.29	57.01	118.92	189.92	0.61

For the samples PG7, PG13 and PG15, that were made with gelatine and biomass, is possible do see that de Young's modulus does not have a direct comparison because it fluctuates. This can be that

there is an ideal proportion of biomass and gelatine that this value is optimized, as it happens with the tensile strength.

The values obtained for the tensile strength and the Young's modulus were not possible to compare with theoretical values, because there are no experiments, like those developed through this work.

4.4.6. Stability tests

This test was only made to the sample PG33. In the study with the different atmospheres, the samples stayed in the balloons for 114 days and they didn't lose any weight, neither colour. On the other hand, when PG33 was left under direct sunlight for 106 days, it shrunk, its colour turned into white and, because it was not covered, it had some black particles, that could come from the test present the room as shown in the figure 68 "PG33 before (left) and after (right) left under direct sunlight".

Figure 68 – PG33 before (left) and after (right) left under direct sunlight.

4.4.7. Moulds

With the sample PG33 it was also done some tests to see if was possible to do some moulds with it. The moulds used were some cupcake moulds, beakers and petri dishes found in the lab. Some experiments were made by pouring the solution directly over the mould. The other method used was to put some solutions into the beaker and then put a smaller beaker or cup into the bigger one and pressing it. However, neither of these methods work to form a mould that holds all the shape. With the first method is possible to notice through the figure 69 "Cupcake mould" that the solution had shrunk, but the side has the wrinkles stamped. In the second method, the solution did not dry completely, but it held the side of the beaker, as shown in the figure 70 "Beaker mould".

Figure 69 – Cupcake mould.

Figure 70 – Beaker mould.

4.5. BG

The sample BG was made following the original experiment, as mentioned in section 3.4.3. The result was a film that is possible to bend, had resistance and is translucid, as seen in the figure 71 “BG after drying”.

Figure 71 – BG after drying.

Next, the sample BG2 was made with gelatine and biomass, following the experiment explained in section 3.4.3., replacing 50 % of the gelatine with biomass. After drying, as shown in the figure 72 “BG2 after drying”, the sample had formed a film that is malleable and homogeneous.

Figure 72 – BG2 after drying.

Whereas, BG3 was made by substituting 80 % of the gelatine by biomass. This sample, before it dried, it was possible to notice that it had a thick texture and after drying it was dense and thick after drying. However, it's still malleable, as shown in the figure 73 "BG3 after drying".

Figure 73 – BG3 after drying.

The final test – BG4 – was made with chitosan, replacing 80 % of the gelatine for chitosan. Before drying the mixture had a foamy look and it's more liquid than the other samples. After drying, this sample had the most different result. It appears to have formed some crystals and didn't form a film, as shown in the figure 74 "BG4 after drying".

Figure 74 – BG4 after drying.

4.5.1. FTIR-ATR

When the FTIR-ATR of the sample's BG (see appendix I.5) are all compared, is possible to see that they are all similar. Between the samples BG2 and BG3, the only difference is the higher intensity of the peaks of BG4 at 1500 cm^{-1}. This difference can occur due to the quantity of biomass used. On the

other hand, in the same wavenumber, BG4 has different peaks, because it was made with chitosan, so it is expected to have a slightly different spectrum.

Identically to the experiment PG three peaks are constant throughout the spectrums. The first peak is located between 3500 and 3100 cm^{-1} and the other two peaks are located at 1660 and 1420 cm^{-1}.

4.6. AMV

Following the original method mentioned in section 3.4.4. was possible to create AMV. The result was a film with a similar texture to a translucid plastic bag that can be found at the supermarket. However, it had some bubbles (see figure 75 “AMV after drying”).

Figure 75 – AMV after drying.

Then, AMV2 was produced by substituting 50 % of the corn-starch for biomass. After two days of drying in the fume hood, with extraction, at room temperature, it stills moist. When dried completely it is crumbly and did not form a film, as shown in the figure 76 “AMV2 after drying”.

Figure 76 – AMV2 after drying.

Finally, the sample AMV3 was made by substituting 80 % of the corn-starch for biomass. The result was the same as AMV2, it was crumbly and didn’t form a film, as shown in the figure 77 “AMV3 after drying”.

Figure 77 – AMV3 after drying.

4.6.1. FTIR-ATR

All the FTIR-ATR spectrums (see appendix I.6) are very similar between them, except for the sample AMV that has an extra peak at 3000 cm^{-1}. This difference can occur, because this sample didn't have any biomass that can react with the other components, making them have different chemical bonds.

To finish, similarly the experiment PG three peaks are constant throughout the spectrums. The first peak is located between 3500 and 3100 cm^{-1} and the other two peaks are located at 1660 and 1420 cm^{-1}.

5. Conclusion and Future Work

The main goal of this work was to develop a bioplastic from an agri-food waste. This goal was achieved by creating a film, however for lack of some tests is not possible to conclude if this bioplastic is biodegradable or not.

The transformation of the biomass to chitosan is not the greenest process, but sometimes by choosing a more environmentally friendly reactant the overall yield of the experiment decreases, making it more costly and less efficient. This can lead to the worst consequences to the environment. [49]

Through the SEM/EDS analysis is possible to conclude that the biomass is very rich in proteins, which is common in chitin. It is also possible to see that all the components of the biomass are present in the chitin and chitosan produced, which is expected. However, is not possible to quantify these components to verify if they are is less quantity in the chitin and chitosan. It is still possible to observe through SEM images that these products have a polymer-like characteristic.

The average degree of deacetylation of the chitosan samples produced is 71.3 %. This value confirms the solubility of the chitosan in dilute acids. However, when the calculation was done with the spectrum FTIR-MIR of the sample Q9 the value obtained was 43.7 %, having a deviation of 39 %. This could have happened because the spectrum FTIR-MIR of Q9 has a lot of noise that can be a consequence of humidity present in the sample or the KBr.

When the TGA analysis was made to the biomass, chitin and chitosan, was possible to conclude that the products became thermally more stable through the treatment. This can entail some benefits, such as, the shelf time of these products can increase. But also, it can have some disadvantages, like not being biodegradable or eco-friendly, like fossil fuel-based plastics.

The first attempt to make a film – the samples FP – was not very successful, because it didn't form a film that could hold is shape after two days at room temperature. Although, when done with commercial chitosan, it may have some interesting applications, but this work aimed to do with the chitosan produced. So, it was not possible to conclude this study.

The method used to produce PG had some successful results. This method used some similar reagents as FP, but by adding the gelatine or agar, as a binder, it made this experiment more efficient. Through the TGA analysis was possible to observe that most of the samples are very degradable, this can be a positive aspect, which can place this film in the biodegradable category. However, as explained earlier, this test was not possible to make. In the SEM images was possible to see that the PG is indeed a cohesive film.

Within the PG tests were possible to produce a strong film and other more flexible and thinner, with chitosan and gelatine. Nevertheless, the first sample had 20 % of the total mass of solids and the second had 80 %. So, it's convenient to try and find a proportion that can offer both options.

Either for the samples with gelatine or with the agar, when there is no polysaccharide added, the tensile strength is higher. Overall, the samples that have agar have a lower tensile strength and there is no direct correlation between the percentage of gelatine in the sample and its tensile strength.

It was possible to do some moulds with these samples, mainly with the sample PG33. However, they did not come in one piece or they didn't dry enough to be in one piece. Therefore, is necessary to create a way to do these moulds more efficiently.

The final experiments were done – BG and AMV – were not as successful as PG, because when substituting part of their components they didn't have the expected results.

For future work, it is important to improve the extraction process from the biomass to the chitosan, in order to have a better yield of all processes. The improvement includes changing the reaction's time and changing some reagents, either for the reaction and for the washing process.

Another suggestion for future work is to improve the proportion of the reagent to improve the flexibility and strength of the film, as well as, test its biodegradability and finally, explore other applications for this chitosan.

6. References

[1] *Science to enable sustainable plastics – A white paper from the 8th Chemical Sciences and Society Summit (C23)*, 2020, rcs.li/sustainable-plastics-report.

[2] Barrett, A. (June 3, 2020). Bioplastics News. *Science to Enable Sustainable Plastics.* Retrieved from July 9, 2020, from https://bioplasticsnews.com/2020/06/03/science-sustainable-plastics/

[3] D'Angelo, G., Elhussieny, A., Faisal, M., Fahim, I., & Everitt, N. (2018). Mechanical Behavior Optimization of Chitosan Extracted from Shrimp Shells as a Sustainable Material for Shopping Bags. *Journal of Functional Biomaterials, 9*(2), 37.

[4] Pal, A. K., & Katiyar, V. (2016). Nanoamphiphilic Chitosan Dispersed Poly(lactic acid) Bionanocomposite Films with Improved Thermal, Mechanical, and Gas Barrier Properties. *Biomacromolecules, 17*(8), 2603–2618.

[5] Narancic, T., Cerrone, F., Beagan, N., & O'Connor, K. E. (2020). Recent Advances in Bioplastics: Application and Biodegradation. *Polymers, 12*(4), 920.

[6] El-Kadi, S.. (2010). *Bioplastic production from inexpensive sources*. VDM Verlag Dr. Müller.

[7] Tsang, Y. F., Kumar, V., Samadar, P., Yang, Y., Lee, J., Ok, Y. S., Song, H., Kim, K.-H., Kwon, E. E., & Jeon, Y. J. (2019). Production of bioplastic through food waste valorization. *Environment International, 127*, 625–644.

[8] (2020) *Technical Platform on the Measurement and Reduction of Food Loss and Waste*. Retrieved from June 2, 2020, from Food and Agriculture Organization of the United Nations: http://www.fao.org/food-loss-and-food-waste/en/

[9] Biscarat, J., Charmette, C., Sanchez, J., & Pochat-Bohatier, C. (2014). Development of a new family of food packaging bioplastics from cross-linked gelatin based films. *The Canadian Journal of Chemical Engineering, 93*(2), 176–182.

[10] *Fact Sheet*. (July, 2018). Retrieved from European Bioplastics: https://docs.european-bioplastics.org/publications/fs/EuBP_FS_What_are_bioplastics.pdf

[11] Yadav, B., Pandey, A., Kumar, L. R., & Tyagi, R. D. (2020). Bioconversion of waste (water)/residues to bioplastics – A circular bioeconomy approach. *Bioresource Technology, 298*, 122584.

[12] Xu, C., Nasrollahzadeh, M., Selva, M., Issaabadi, Z., & Luque, R. (2019). Waste-to-wealth: biowaste valorization into valuable bio(nano)materials. *Chemical Society Reviews, 48*(18), 4791–4822.

[13] Deshmukh, K., Basheer Ahamed, M., Deshmukh, R. R., Khadheer Pasha, S. K., Bhagat, P. R., & Chidambaram, K. (2017). Biopolymer Composites With High Dielectric Performance: Interface Engineering. *Biopolymer Composites in Electronics*, 27–128.

[14] Gowman, A., Picard, M., Lim, L.-T., Misra, M., & Mohanty, A. (2019). Fruit Waste Valorization for Biodegradable Biocomposite Applications: A Review. *BioResources, 14*(4), 10047-10092.

[15] Ruiz, C., Kenny, S. T., Narancic, T., Babu, R., & Connor, K. O. (2019). Conversion of waste cooking oil into medium chain polyhydroxyalkanoates in a high cell density fermentation. *Journal of Biotechnology, 306*, 9–15.

[16] Dietrich, K., Dumont, M.-J., Del Rio, L. F., & Orsat, V. (2017). Producing PHAs in the bioeconomy — Towards a sustainable bioplastic. *Sustainable Production and Consumption, 9*, 58–70.

[17] *What are bioplastics?* (n.d.) Retrieved July 10, 2020, from European bioplastics: https://www.european-bioplastics.org/bioplastics/

[18] Fahim, I. S., Chbib, H., & Mahmoud, H. M. (2019). The synthesis, production & economic feasibility of manufacturing PLA from agricultural waste. *Sustainable Chemistry and Pharmacy, 12*, 100142.

[19] Melnyk, L., Kubatko, O., Piven, V., Kucherenko, P., & Ihnatchenko, V. (2019). Bioplastics production for circular economy and sustainable development promotion. *Ekonomika APK, 11*, 79–84.

[20] *Bioplastic market data.* (n.d.) Retrieved July 10, 2020, from European bioplastics: https://www.european-bioplastics.org/market/

[21] Fricke, A. (2018, January 8). *Plastic waste - or resource?* Retrieved July 10, 2020, from Newtrients: https://newtrients.ucc.ie/plastic-waste-resource/

[22] *Compostable Plastics* (December 2, 2017). Retrieved July 10, 2020, from World Centric: https://www.worldcentric.com/blog/compostable-plastics

[23] *Waste management and recovery options for bioplastics.* (n.d.) Retrieved July 10, 2020, from European bioplastics: https://www.european-bioplastics.org/bioplastics/waste-management/

[24] *How much agricultural area is used for bioplastics?* (n.d.) Retrieved July 10, 2020, from European bioplastics: https://www.european-bioplastics.org/bioplastics/waste-management/

[25] Issbrücker, C. (February 28, 2018) *How much land do we really need to produce bio-based plastics?* Retrieved July 10, 2020, from European bioplastics: https://www.european-bioplastics.org/how-much-land-do-we-really-need-to-produce-bio-based-plastics/

[26] Reim, W., Parida, V., & Sjödin, D. R. (2019). Circular Business Models for the Bio-Economy: A Review and New Directions for Future Research. *Sustainability, 11*(9), 2558.

[27] *Market drivers and development.* (n.d.) Retrieved July 10, 2020, from European bioplastics: https://www.european-bioplastics.org/market/market-drivers/

[28] Verma, D., & Fortunati, E. (2019). Biopolymer processing and its composites. *Biomass, Biopolymer-Based Materials, and Bioenergy*, 3–23.

[29] Casadidio, C., Peregrina, D. V., Gigliobianco, M. R., Deng, S., Censi, R., & Di Martino, P. (2019). Chitin and Chitosans: Characteristics, Eco-Friendly Processes, and Applications in Cosmetic Science. *Marine Drugs, 17*(6), 369.

[30] Rouhani Shirvan, A., Shakeri, M., & Bashari, A. (2019). Recent advances in application of chitosan and its derivatives in functional finishing of textiles. *The Impact and Prospects of Green Chemistry for Textile Technology*, 107–133.

[31] Ifuku, S., Morooka, S., Norio Nakagaito, A., Morimoto, M., & Saimoto, H. (2011). Preparation and characterization of optically transparent chitin nanofiber/(meth)acrylic resin composites. *Green Chemistry, 13*(7), 1708.

[32] Kumar, S., Ye, F., Dobretsov, S., & Dutta, J. (2019). Chitosan Nanocomposite Coatings for Food, Paints, and Water Treatment Applications. *Applied Sciences, 9*(12), 2409.

[33] Mishra, R. K., Ha, S. K., Verma, K., & Tiwari, S. K. (2018). Recent progress in selected bio-nanomaterials and their engineering applications: An overview. *Journal of Science: Advanced Materials and Devices, 3*(3), 263–288.

[34] Duan, B., Huang, Y., Lu, A., & Zhang, L. (2018). Recent advances in chitin based materials constructed via physical methods. *Progress in Polymer Science, 82*, 1–33.

[35] Nessa, F., Masum, S., Asaduzzaman, M., Roy, S., Hossain, M., & Jahan, M. (2010). A Process for the Preparation of Chitin and Chitosan from Prawn Shell Waste. *Bangladesh Journal of Scientific and Industrial Research, 45*(4), 323-330.

[36] Liu, S. (2017). An Overview of Biological Basics. *Bioprocess Engineering*, 21–80.

[37] Elhussieny, A., Faisal, M., D'Angelo, G., Aboulkhair, N. T., Everitt, N. M., & Fahim, I. S. (2020). Valorisation of shrimp and rice straw waste into food packaging applications. *Ain Shams Engineering Journal*.

[38] Molnár, Á. (2019). The use of chitosan-based metal catalysts in organic transformations. *Coordination Chemistry Reviews, 388*, 126–171.

[39] Azevedo, A. R., Almeida, V. M., & Santos, S. A. S.. (2018). Síntese de bioplásticos feitos com polímeros naturais: uma alternativa para a gestão ambiental. *Conhecimento & Diversidade, 9*(19), 59-17.

[40] Malajovic, M. A. (n.d.). BioTecnologia: ensino e divulgação. *Guia 46 - Bioplásticos: plásticos de gelatina*. Retrieved from April 17, 2020, from https://bteduc.com/guias.html

[41] Wild, D. (2018, June 24). *Food for thought - Your DIY guide for creating bioplastics.* Retrieved from April 17, 2020, from http://www.daniellewilde.com/wp-content/uploads/2018/10/SDU-Design_FoodForThought_24June2018.pdf

[42] Harris, R., Ahrenstorff, C., Theryo, G., Johnson, A., & Wissinger, J. (2017). *Make it and Break it: Bioplastics from Plant Starch with incorporation of Engineering Practices.* University of Minnesota. Retrieved from https://csp.umn.edu/wp-content/uploads/2017/03/Make-it-and-Break-it.pdf

[43] Laboratory testing inc. (n.d.). *Scanning Electron Microscopy.* Retrieved April 17, 2020, from https://www.labtesting.com/services/materials-testing/metallurgical-testing/sem-analysis/

[44] Heidaria, F., Razavib, M., Bahrololoomd, M. E., Tahririe, M., Rasoulianboroujenie, M., Koturif, H. & Tayebie, L. (December 26, 2016) Preparation of natural chitosan from shrimp shell with different deacetylation degree. *Material research innovations, 22*(3), 177–181.

[45] Chen, Y., Zou, C., Mastalerz, M., Hu, S., Gasaway, C., & Tao, X. (2015). Applications of Micro-Fourier Transform Infrared Spectroscopy (FTIR) in the Geological Sciences — A Review. *International Journal of Molecular Sciences, 16*(12), 30223–30250.

[46] Groenewoud, W. M. (2001). Thermogravimetry. *Characterisation of Polymers by Thermal Analysis*, 61–76.

[47] Gbenebor, O. P., Adeosun, S. O., Lawal, G. I., Jun, S., & Olaleye, S. A. (2017). Acetylation, crystalline and morphological properties of structural polysaccharide from shrimp exoskeleton. *Engineering Science and Technology, an International Journal, 20*(3), 1155–1165.

[48] Andrade, S. M. B. de, Ladchumananandasivam, R., Rocha, B. G. da, Belarmino, D. D., & Galvão, A. O. (2012). The Use of Exoskeletons of Shrimp (Litopenaeus vanammei) and Crab (Ucides cordatus) for the Extraction of Chitosan and Production of Nanomembrane. *Materials Sciences and Applications, 03*(07), 495–508.

[49] Houlton, S. (2019, September). A better solution for the environment. *Chemistry world, 16*(9), 20-21.

Appendix I – FTIR-ATR spectrums

Appendix I.1 – FTIR-ATR spectrums of chitin

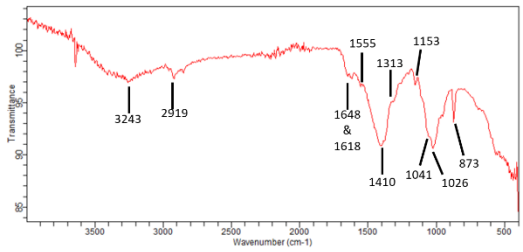

Figure A1 - FTIR-ATR spectra of the C1.

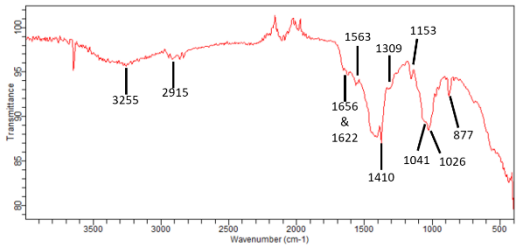

Figure A2 - FTIR-ATR spectra of the C2.

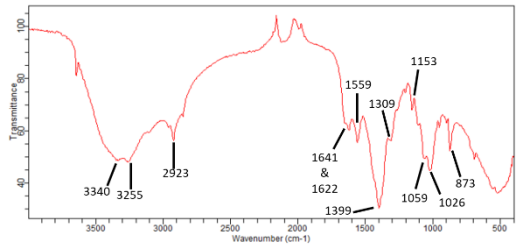

Figure A3 - FTIR-ATR spectra of the C3.

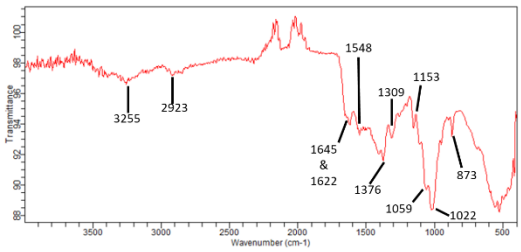

Figure A4 - FTIR-ATR spectra of the C4.

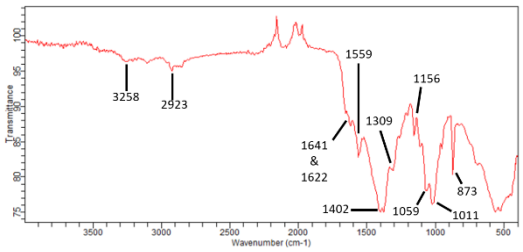

Figure A5 - FTIR-ATR spectra of the C5.

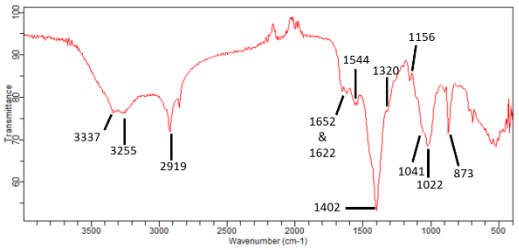

Figure A6 - FTIR-ATR spectra of the C6.

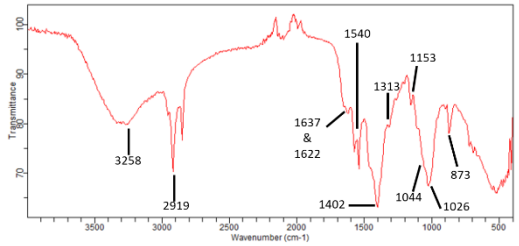

Figure A7 - FTIR-ATR spectra of the C7.

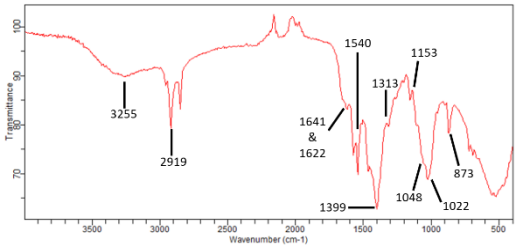

Figure A8 - FTIR-ATR spectra of the C8.

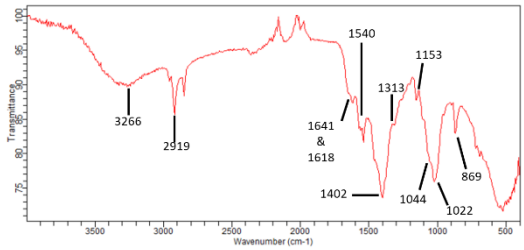

Figure A9°° - FTIR-ATR spectra of the C9.

Appendix I.2 – FTIR-ATR spectrums of chitosan

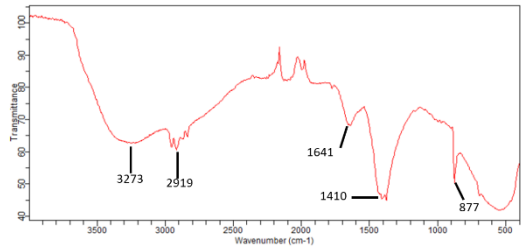

Figure B1- FTIR-ATR spectra of the Q1.b.

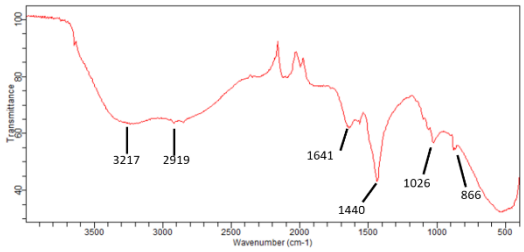

Figure B2 - FTIR-ATR spectra of the Q1.p.

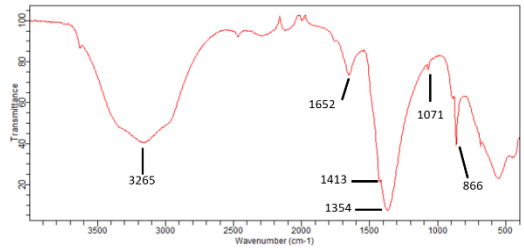

Figure B3 - FTIR-ATR spectra of the Q1.p after 2 weeks drying.

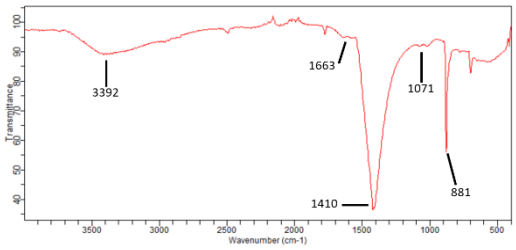

Figure B4 - FTIR-ATR spectra of the Q2.b.

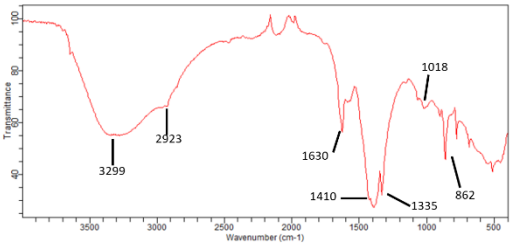

Figure B5 - FTIR-ATR spectra of the Q2.b.

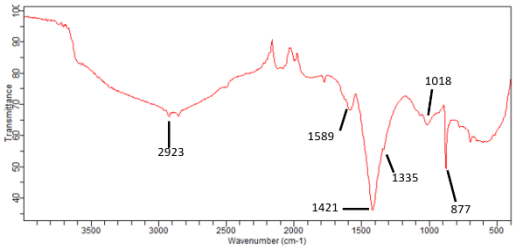

Figure B6 - FTIR-ATR spectra of the Q3.

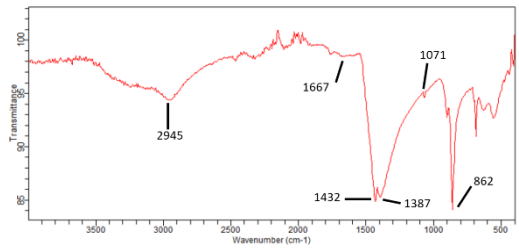

Figure B7 - FTIR-ATR spectra of the Q4.b.

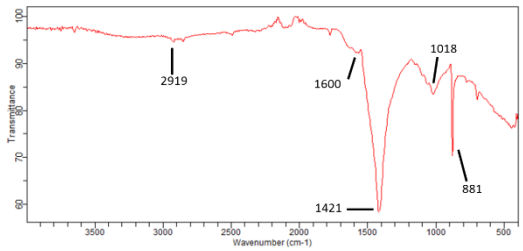

Figure B8 - FTIR-ATR spectra of the Q4.e.

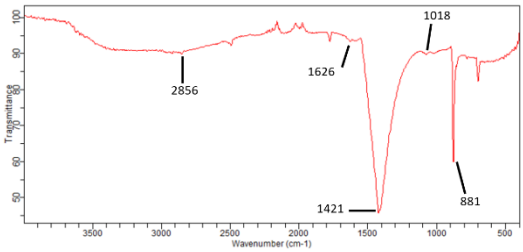

Figure B9 - FTIR-ATR spectra of the Q5.

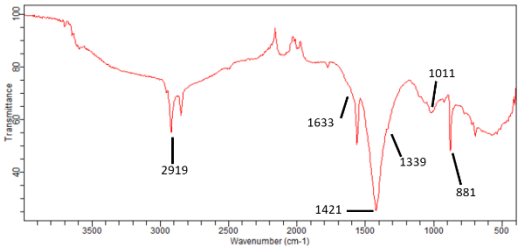

Figure B10 - FTIR-ATR spectra of the Q8.

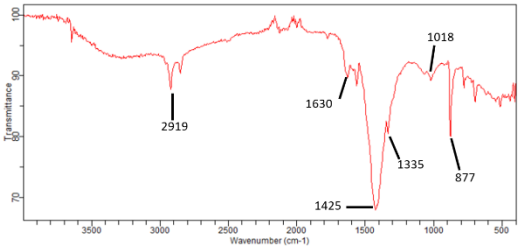

Figure B11 - FTIR-ATR spectra of the Q9.

Appendix I.3 – FTIR-ATR spectrums of FP

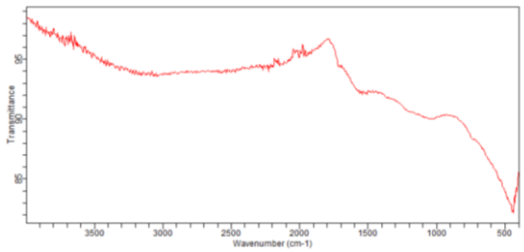

Figure C1 - FTIR-ATR spectra of the FP1.

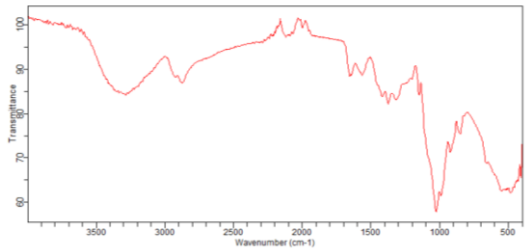

Figure C2 - FTIR-ATR spectra of the FP2 after drying in the muffle.

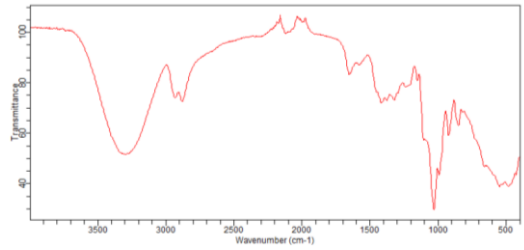

Figure C3 - FTIR-ATR spectra of the FP2 after drying in the stove.

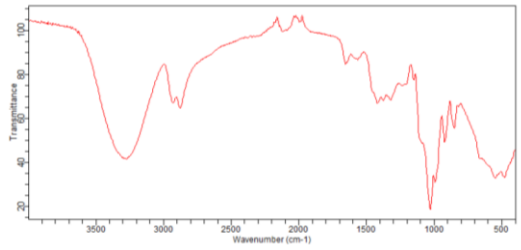

Figure C4 - FTIR-ATR spectra of the FP4.

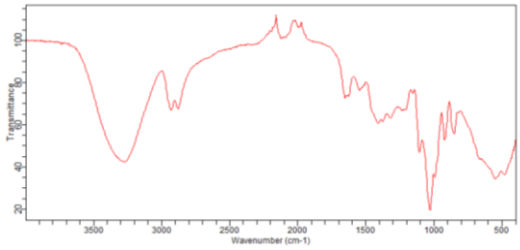

Figure C5 - FTIR-ATR spectra of the FP5 after drying 1 h in the muffle.

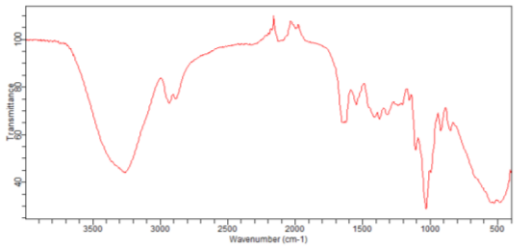

Figure C6 - FTIR-ATR spectra of the FP5 after drying 2 h in the muffle.

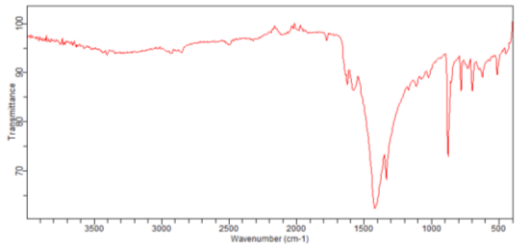

Figure C7 - FTIR-ATR spectra of the FP6 after drying 1 day in the stove.

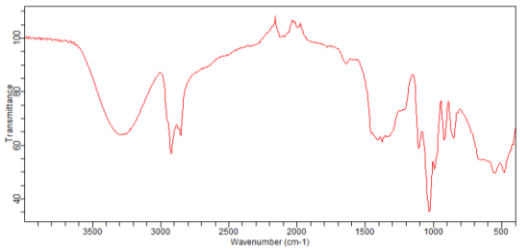

Figure C8 - FTIR-ATR spectra of the FP after drying 1 week in the stove.

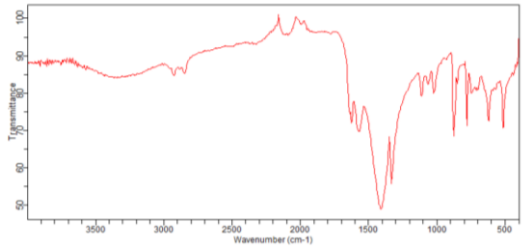

Figure C9 - FTIR-ATR spectra of the FP7 after 1 day drying in the stove.

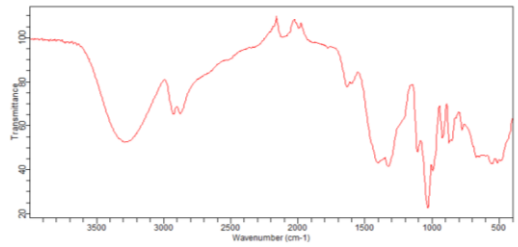

Figure C10 - FTIR-ATR spectra of the FP7 after drying 1 week in the stove.

Figure C11 - FTIR-ATR spectra of the FP8.

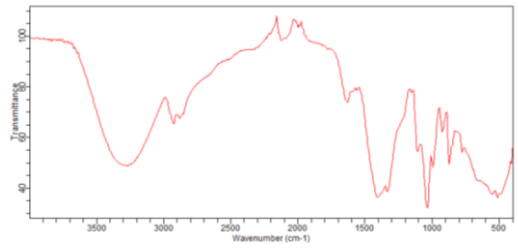

Figure C12 - FTIR-ATR spectra of the FP9.

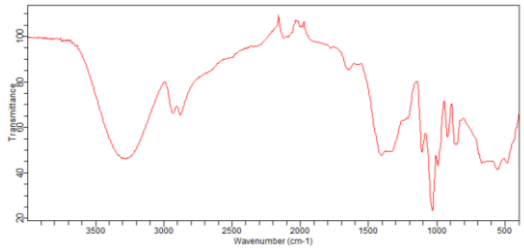

Figure C13 - FTIR-ATR spectra of the FP10.

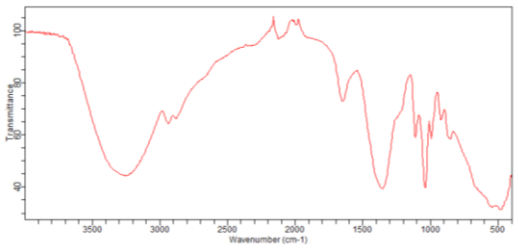

Figure C14 - FTIR-ATR spectra of the FP10 after 2 days at room temperature.

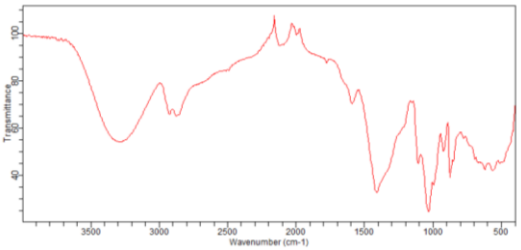

Figure C15- FTIR-ATR spectra of the FP11.

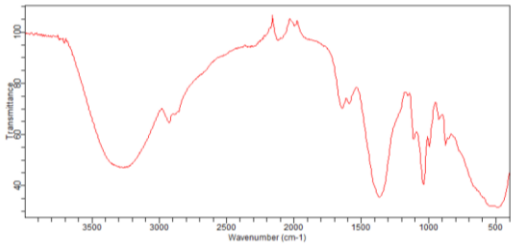

Figure C16 - FTIR-ATR spectra of the FP11 after 2 days at room temperature.

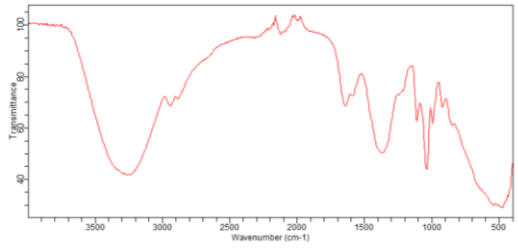

Figure C17 - FTIR-ATR spectra of the FP12.

Appendix I.4 – FTIR-ATR spectrums of PG

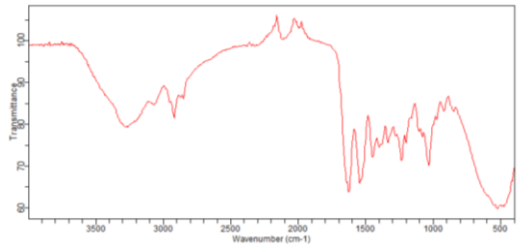

Figure D1 - FTIR-ATR spectra of the PG1.

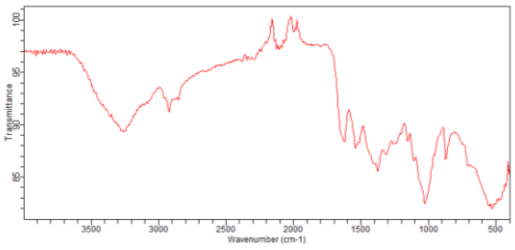

Figure D6 - FTIR-ATR spectra of the PG6.

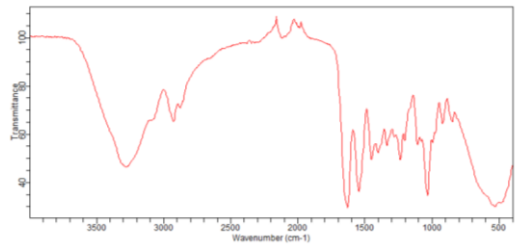

Figure D2 - FTIR-ATR spectra of the PG2.

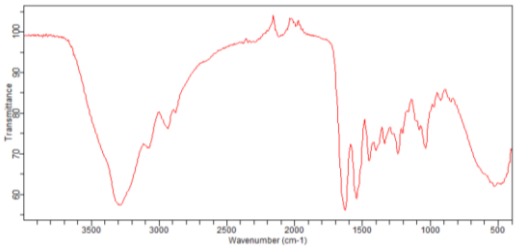

Figure D7 - FTIR-ATR spectra of the PG7.

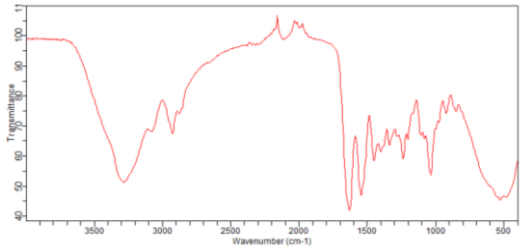

Figure D3 - FTIR-ATR spectra of the PG3.

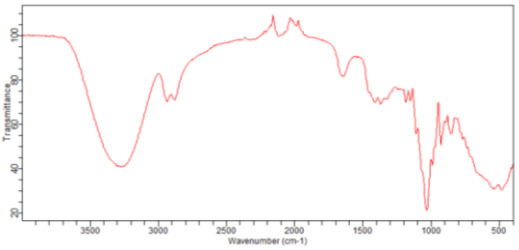

Figure D8 - FTIR-ATR spectra of the PG8.

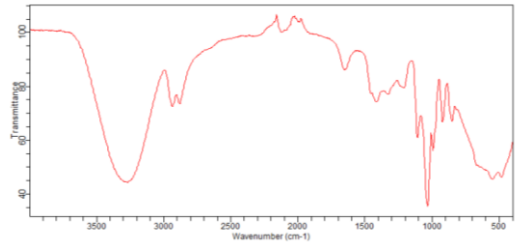

Figure D4 - FTIR-ATR spectra of the PG4.

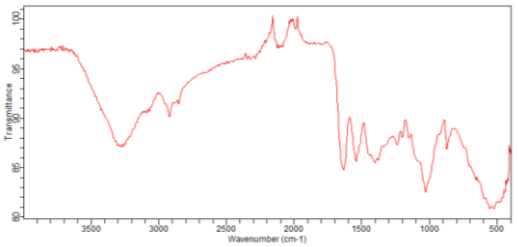

Figure D9 - FTIR-ATR spectra of the PG9.

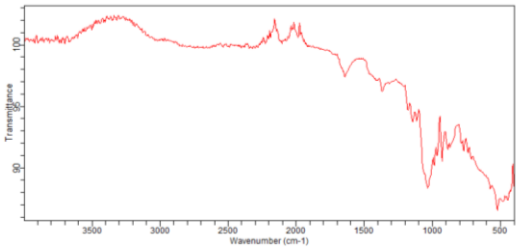

Figure D5 - FTIR-ATR spectra of the PG5.

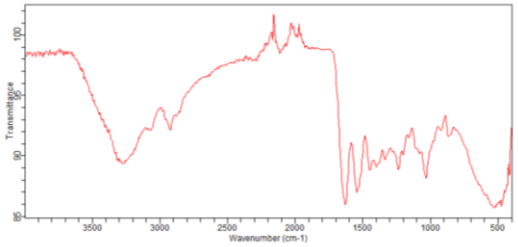

Figure D10 - FTIR-ATR spectra of the PG10.

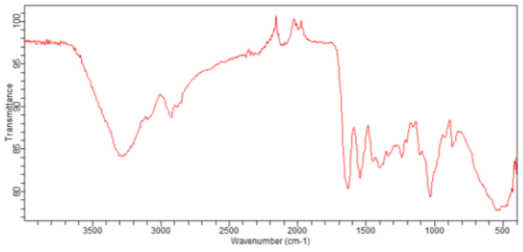

Figure D11 - FTIR-ATR spectra of the PG11.

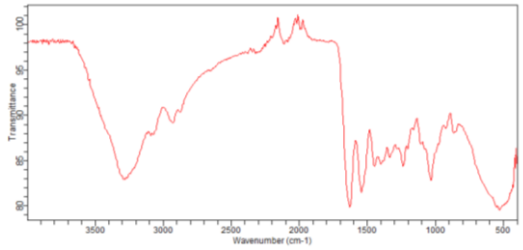

Figure D12 - FTIR-ATR spectra of the PG12.

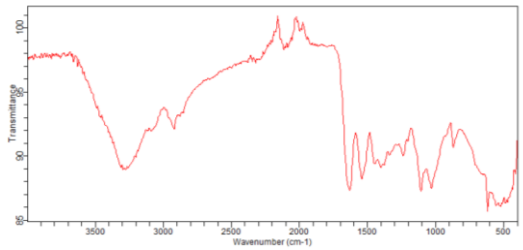

Figure D13 - FTIR-ATR spectra of the PG13.

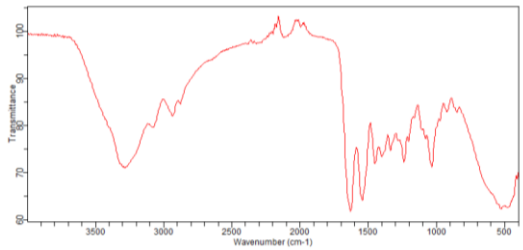

Figure D14 - FTIR-ATR spectra of the PG14.

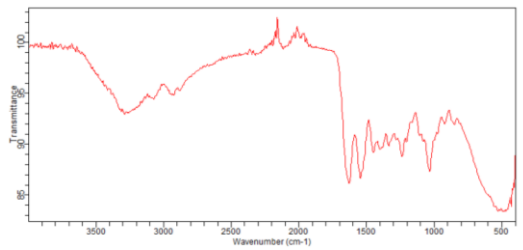

Figure D15 - FTIR-ATR spectra of the PG15.

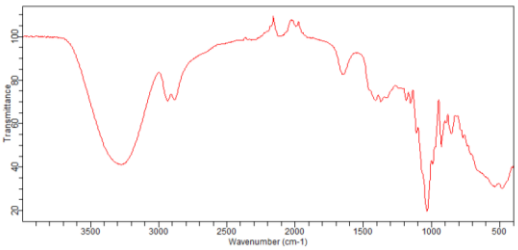

Figure D16 - FTIR-ATR spectra of the PG16.

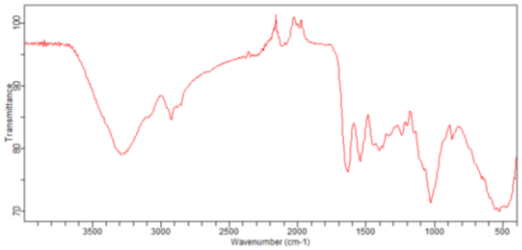

Figure D17 - FTIR-ATR spectra of the PG17.

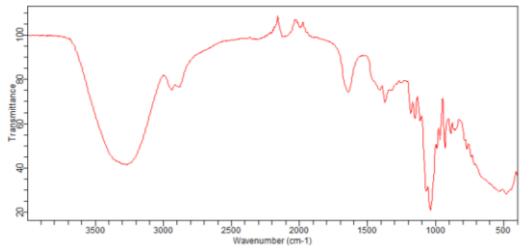

Figure D18 - FTIR-ATR spectra of the PG18.

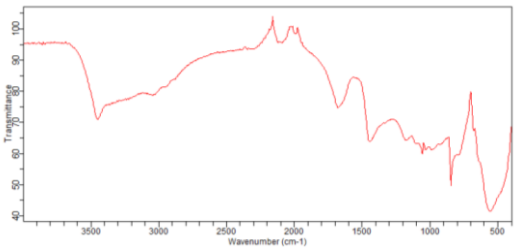

Figure D19 - FTIR-ATR spectra of the PG19.

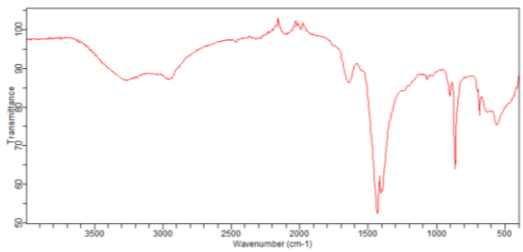

Figure D20 - FTIR-ATR spectra of the PG19.d.

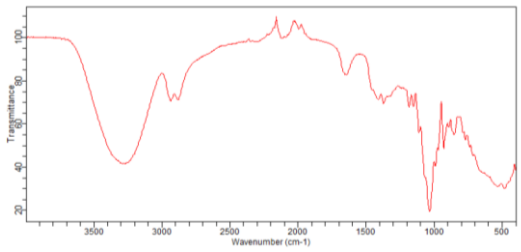

Figure D21 - FTIR-ATR spectra of the PG20.

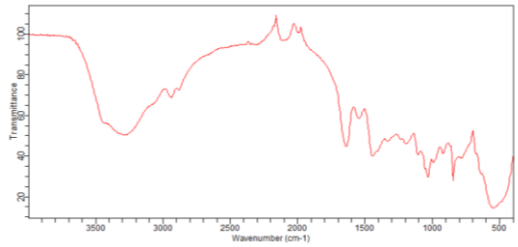

Figure D22 - FTIR-ATR spectra of the PG21.

Figure D23 - FTIR-ATR spectra of the PG22.

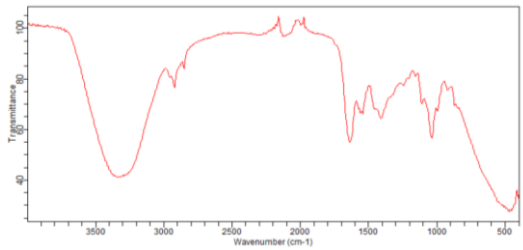

Figure D24 - FTIR-ATR spectra of the PG23.

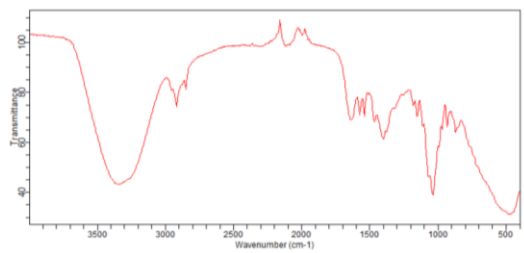

Figure D25 - FTIR-ATR spectra of the PG24.

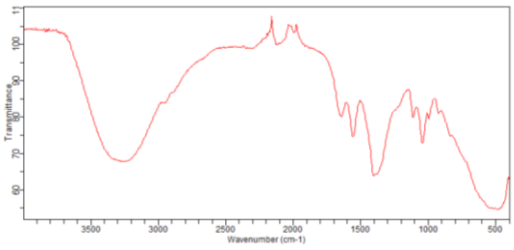

Figure D26 - FTIR-ATR spectra of the PG25.

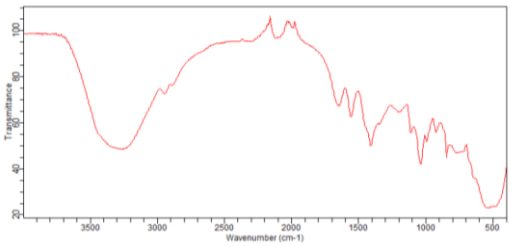

Figure D27 - FTIR-ATR spectra of the PG26.f.

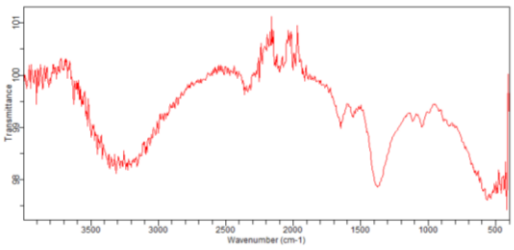

Figure D28 - FTIR-ATR spectra of the PG26.c.

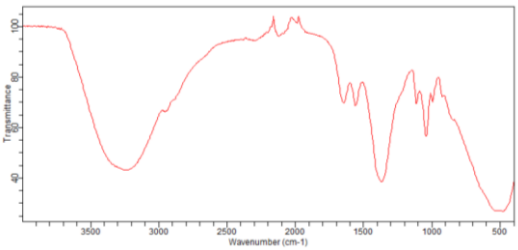

Figure D29 - FTIR-ATR spectra of the PG26.g.

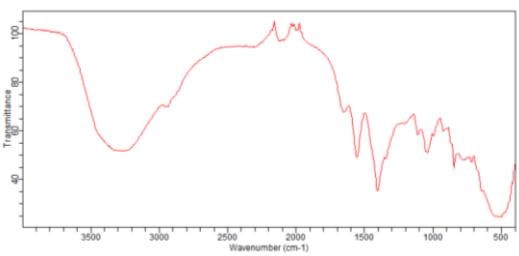

Figure D30 - FTIR-ATR spectra of the PG27.

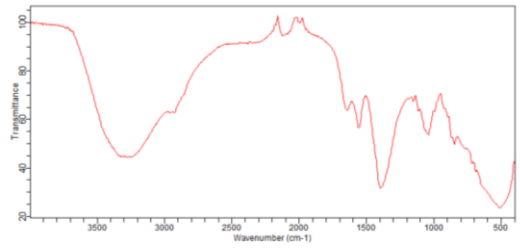

Figure D31 - FTIR-ATR spectra of the PG28.

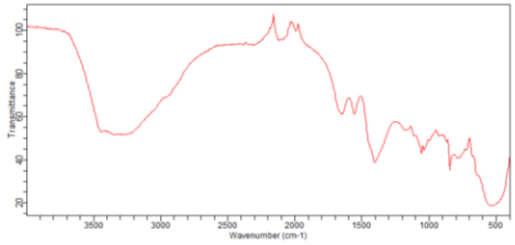

Figure D32 - FTIR-ATR spectra of the PG29.

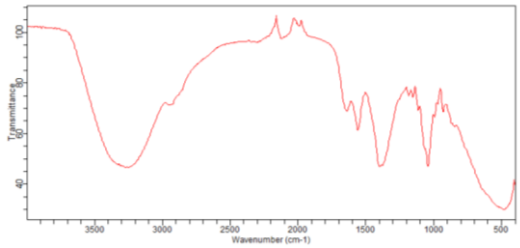

Figure D33 - FTIR-ATR spectra of the PG30.

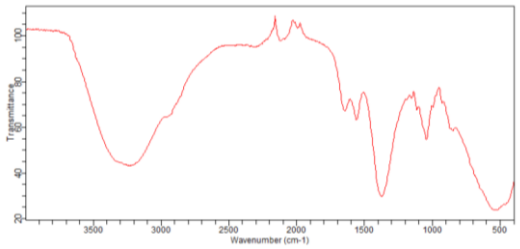

Figure D34 - FTIR-ATR spectra of the PG31.

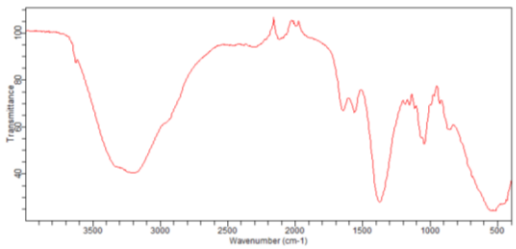

Figure D35 - FTIR-ATR spectra of the PG31.c.

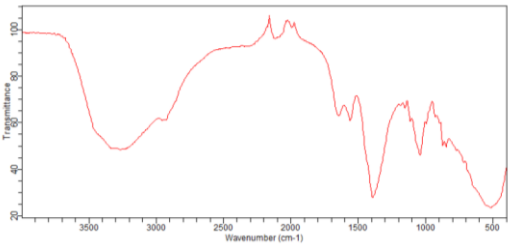

Figure D36 - FTIR-ATR spectra of the PG32.

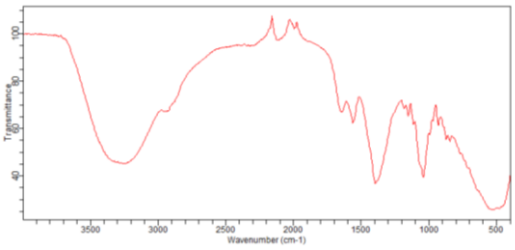

Figure D37 - FTIR-ATR spectra of the PG32.c.

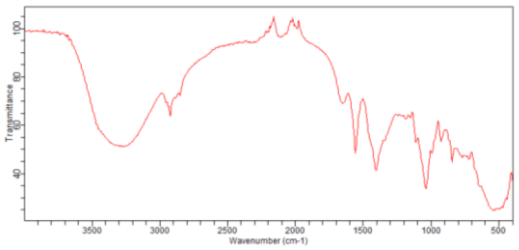

Figure D38 - FTIR-ATR spectra of the PG33.

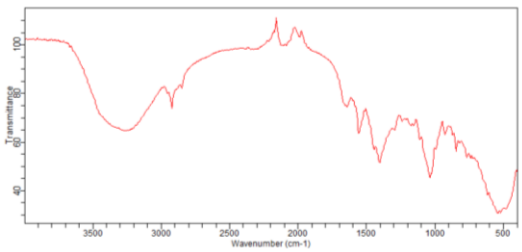

Figure D39 - FTIR-ATR spectra of the PG33.2.

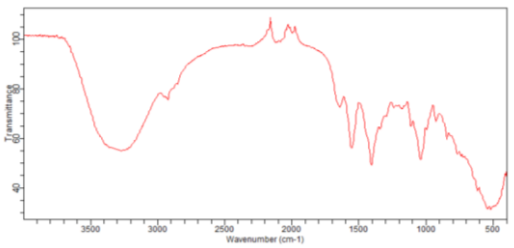

Figure D40 - FTIR-ATR spectra of the PG33.3.

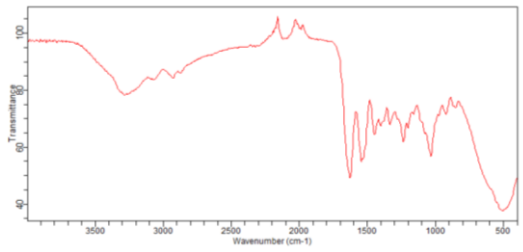

Figure D41 - FTIR-ATR spectra of the PG34.

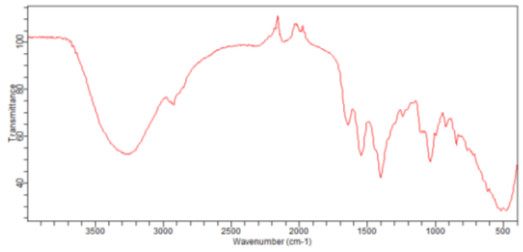

Figure D42 - FTIR-ATR spectra of the PG35.

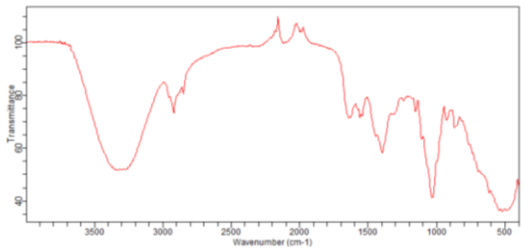

Figure D43 - FTIR-ATR spectra of the PG36.

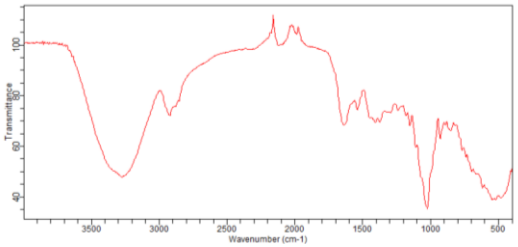

Figure D44 - FTIR-ATR spectra of the PG37.

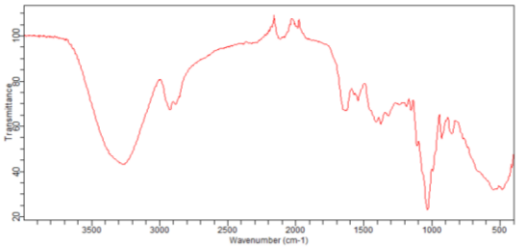

Figure D45 - FTIR-ATR spectra of the PG37.2.

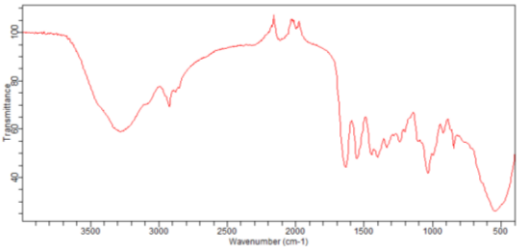

Figure D46 - FTIR-ATR spectra of the PG38.

Appendix I.5 – FTIR-ATR spectrums of BG

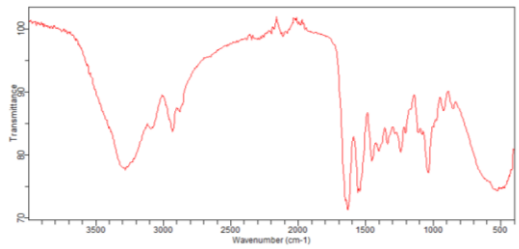

Figure E1 - FTIR-ATR spectra of the BG.

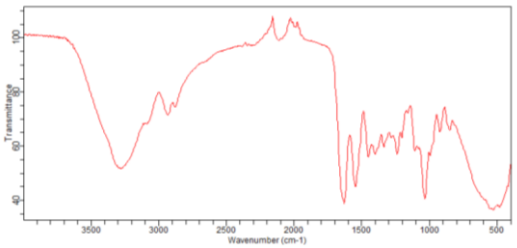

Figure E2 - FTIR-ATR spectra of the BG2.

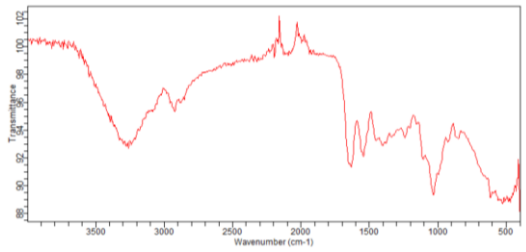

Figure E3 - FTIR-ATR spectra of the BG3.

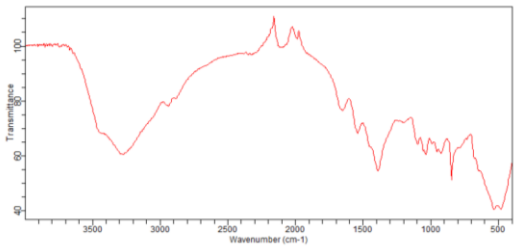

Figure E4 - FTIR-ATR spectra of the BG4.

Appendix I.6 – FTIR-ATR spectrums of AMV

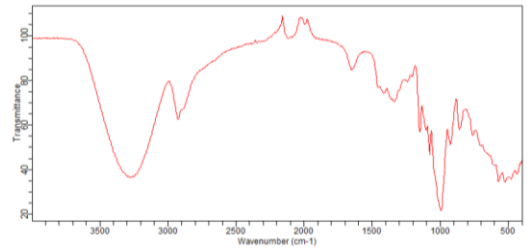

Figure F1 - FTIR-ATR spectra of the AMV.

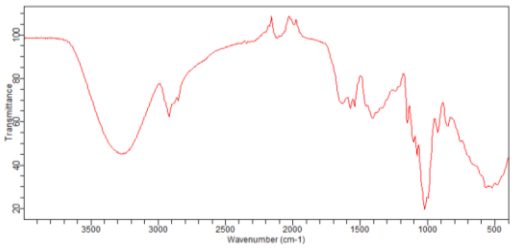

Figure F3 - FTIR-ATR spectra of the AMV3.

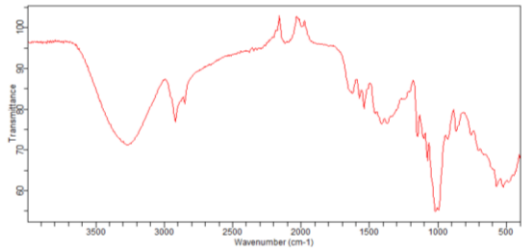

Figure F2 - FTIR-ATR spectra of the AMV2.